

**Theory of photon statistics and optical coherence in a multiple-scattering random-laser medium**

Lucia Florescu and Sajeev John

*Department of Physics, University of Toronto, Toronto, Ontario, Canada M5S 1A7*

(Received 26 September 2003; published 14 April 2004)

We derive the photon-number probability distribution and the resulting degree of second-order optical coherence for light emission from a uniformly distributed active species within a multiple-light-scattering medium. This is obtained from a master equation describing the probability distribution for photons in the vicinity of position  $\mathbf{r}$ , traveling with a wave vector  $\mathbf{k}$ , related, in turn, to a coarse-grained average of the optical Wigner coherence function. Using a simple model for isotropic, spatially uncorrelated scatterers, this reduces to a generalization of the master equation of a conventional laser in which the medium behaves like a random collection of low-quality factor cavities that are coupled by photon diffusion between a given cavity and its neighbors. Laserlike coherence, on average, is obtained in the random laser above a specific pumping threshold. Photon-number statistics above and below the lasing threshold are computed by first assuming that the atomic response to the local electromagnetic fields is nearly instantaneous. Corrections to this simple model, arising from nonadiabatic atomic dynamics, are then estimated. The dependence of the photon statistics on scatterer density, gain concentration, and position within a sample reveal that, on average, increase of the scattering strength (decrease of the photon transport mean free path) in the medium leads to a sharper peak in the local photon-number distribution, characteristic of increased local coherence in the optical field. We also evaluate the coherence of the output field at points outside the random-laser medium. This is a weighted average of radiation emitted at different positions in the sample, exhibiting varying degrees of coherence due to variations in the local pumping intensity.

DOI: 10.1103/PhysRevE.69.046603

PACS number(s): 42.55.Zz, 42.25.Dd, 42.55.Ah

**I. INTRODUCTION**

The prediction [1] and observation [2] of laserlike emission from multiple-light-scattering media with gain have provided a compelling starting point for the investigation of disordered dielectric microstructures as alternative sources of coherent light emission. Numerous experimental studies of the emission carried out in colloidal samples [3–6] and optically [7] and electrically [8] pumped semiconductor powders have confirmed that the emission from these multiple-light-scattering dielectric microstructures exhibits spectral and temporal properties characteristic of a multimode laser oscillator. These observations include the existence of a well-defined threshold pump intensity above which the emission at particular frequencies increases more rapidly with pump intensity than below threshold and the concomitant collapse of the emission linewidth and pulse duration shortening. More recent experiments [9,10] have demonstrated, for the first time, that light emitted from random amplifying media, above this threshold, exhibits coherence properties characteristic of true laser light.

A number of theoretical models have been developed to describe lasing in random media. Specific experimental features of the spectral and temporal properties of the emission can be explained by the ring laser model [5], diffusion models [11] describing the random walk of photons [12], and one-dimensional models [13] based on the time-dependent Maxwell-Bloch equations. None of these models, however, has treated the coherence properties of the emitted light. Traditionally, the photon statistics of a laser has been investigated using two distinct but equivalent methods [14]. One is based on the Langevin noise operator formalism and the other is based on a master equation approach. Early theoret-

ical models [15,16] developed to investigate the radiation statistics of a random laser applied the Langevin approach (Boltzmann-Langevin equation for photons), adapted to the case of a random amplifying medium. However, the presence of a diffusion term in the equation describing the fluctuations of the photon number made it difficult to apply this approach to nonlinear systems. Due to the presence of the nonlinear coupling between the atomic and radiation variables, an analytical solution was not obtained. On the other hand, a direct numerical solution is complicated due to the presence of Langevin noise operators. As a result, the photon statistics was investigated only for a system approaching the laser threshold from below. Recently [17], some moments of the photon distribution of a random laser were evaluated, using a model for the “chaotic” nature of the cavity modes (described by a random cavity escape rate), combined with a master equation formalism. However, this study did not evaluate higher order factorial moments of the photon-number distribution, essential to understanding the emission coherence properties. The fluctuation properties of the radiation of a random laser, modeled as a chaotic cavity, have also been considered [18] using a noise-operator formalism and a full nonadiabatic treatment of the nonlinear response of the atomic system.

In this paper, we derive the coherence properties of the random laser using a simple approach, based on the master equation formalism, generalized to describe ensemble-averaged transport properties of light in a multiple-light-scattering medium. This makes use of a rate equation model for the light emitting atoms in the medium, known to provide an accurate picture of the laser operation for both conventional and random lasers. In previous work [11], the emission of radiation in random amplifying media is described by a

set of position-dependent generalized laser equations for the optical energy density and the atomic populations. Here, the multiple-scattering character of the transport is described by a diffusion term that replaces the cavity-loss term in a conventional laser. The rate equations include a spontaneous emission term that partially accounts for the quantum fluctuations. However, this formalism does not describe the coherence properties of the emission, since it does not incorporate the probabilistic character of the photon emission and absorption processes. Photon statistics and probability can be described using a birth-death (master) equation for photon distribution function [19]. Such an equation should reproduce, at least in some order of approximation, the rate equations for average optical energy density and atomic population. In our study, we generalize the master equation for photon statistics in a conventional laser to the case of a random laser by replacing the cavity-loss terms by terms that describe radiative transfer and multiple light scattering. This is obtained from a microscopic analysis of the nonlinear wave equation for electromagnetic transport, in which the nonlinearities are treated in a simple mean-field approximation and transport is described in an ensemble-averaged wave diffusion approximation. This description attributes feedback and laser activity to wave transport mediated by highly probable realizations of the scattering potential represented by the ensemble-averaged diffusion coefficient. In reality, there may be large local fluctuations about the average which also contribute to lasing at a local pump threshold that is considerably less than average pump threshold for the entire medium. These highly improbable configurations of the random medium may cause isolated regions of a large sample to exhibit lasing prior to the entire medium [20]. In our mean-field theory, we neglect these highly improbable, “localized” contribution. Our model leads to a set of generalized master equations for photons at different positions within the sample, and allows evaluation of the average emission coherence. This model enables direct description of the system in terms of the experimentally defined parameters, such as scatterer density and gain concentration.

The paper is organized as follows. In Sec. II, we review the multiple-light-scattering theory of light in random amplifying media. In Sec. III, we derive the master equation for a random laser. The master equation is solved in the steady-state limit by adiabatically eliminating the atomic degrees of freedom in Sec. IV. Here, we calculate the photon distribution function for spatial modes inside the sample. The photon statistics for light emitted inside the sample as well as for light measured by a detector outside the sample is then computed in Sec. V. In Sec. VI, we present a qualitative physical interpretation of the numerical results obtained. In Sec. VII, we discuss the effects of nonadiabaticity of the atomic response in the “bad cavity” regime, and in Sec. VIII we present concluding remarks.

## II. MEAN-FIELD THEORY FOR WAVE PROPAGATION IN RANDOM AMPLIFYING MEDIA

The physical system we study consists of a random dielectric medium uniformly doped with resonant atoms. The

atomic system is incoherently pumped by a monochromatic optical beam. For intense optical pulses containing many photons, the quantum mechanical nature [21] of the electromagnetic field is neglected, and a semiclassical treatment of the radiation is adequate. In this case, the coupled atom-field system is described by the Maxwell-Bloch equations [22]. For simplicity, we consider a scalar field  $E(\mathbf{r}, t)$  which we associate with the electric field of light. It is expected [23] that in the multiple-scattering regime the vector nature of the electromagnetic field becomes unimportant, as the scattered light becomes depolarized. The propagation of the electromagnetic radiation through the nonlinear optical medium is described by the scalar wave equation

$$\nabla^2 E(\mathbf{r}, t) - \frac{\epsilon_1(\mathbf{r})}{c^2} \frac{\partial^2 E(\mathbf{r}, t)}{\partial t^2} = \frac{4\pi}{c^2} \frac{\partial^2 P_{nl}^{atoms}(\mathbf{r}, t)}{\partial t^2}. \quad (2.1)$$

Here,  $\epsilon_1(\mathbf{r})$  is a randomly varying *linear* dielectric function, whereas  $P_{nl}^{atoms}(\mathbf{r}, t)$  describes the *nonlinear* macroscopic polarization density of the medium due to presence of resonant atoms.

The linear dielectric function

$$\epsilon_1(\mathbf{r}) = \epsilon_0 + \epsilon_{fluct}(\mathbf{r}) \quad (2.2)$$

has an average value  $\epsilon_0$  and a randomly fluctuating part  $\epsilon_{fluct}(\mathbf{r})$ , which satisfies  $\langle \epsilon_{fluct}(\mathbf{r}) \rangle_{ens} = 0$ . Here,  $\langle \rangle_{ens}$  denotes a statistical averaging over all possible realizations of the dielectric microstructure. We note that  $\epsilon_{fluct}(\mathbf{r})$  is linear and in general complex, and may account for inhomogeneous linear absorption effects.

The nonlinear polarization due to the amplifying medium can be expressed (after an adiabatic treatment of the atomic system) as [22]

$$P_{nl}^{atoms}(\mathbf{r}) = \chi(\mathbf{r})E(\mathbf{r}). \quad (2.3)$$

Here, the complex optical susceptibility  $\chi(\mathbf{r})$  is given by

$$\chi(\mathbf{r}) = \chi_0 \Delta N(\mathbf{r})/V. \quad (2.4)$$

$\chi_0$  is a complex quantity which depends on the detailed microscopic characteristics of the gain medium [24].  $\Delta N(\mathbf{r})$  is the local atomic population inversion (difference in population of atoms in the excited state and ground state of the laser transition).  $\Delta N(\mathbf{r})$  depends on the pumping rate  $\mathcal{P}(\mathbf{r})$  (which determines the excitation rate and which decreases with depth from the sample surface due to both absorption and scattering) and the emission field intensity  $|E(\mathbf{r})|^2$  (which governs stimulated emission). Here, we model the gain medium as a four-level system (see Fig. 1), in which the laser transition takes place between levels  $|3\rangle$  and  $|2\rangle$ . We also assume that levels  $|4\rangle$  and the lower level of the laser transition,  $|2\rangle$ , are unpopulated due to rapid decay to lower levels. In this case, the population inversion is given by [22]

$$\Delta N(\mathbf{r}) = \frac{\mathcal{P}(\mathbf{r})}{1 + \frac{|E(\mathbf{r})|^2}{I_{sat}}}. \quad (2.5)$$

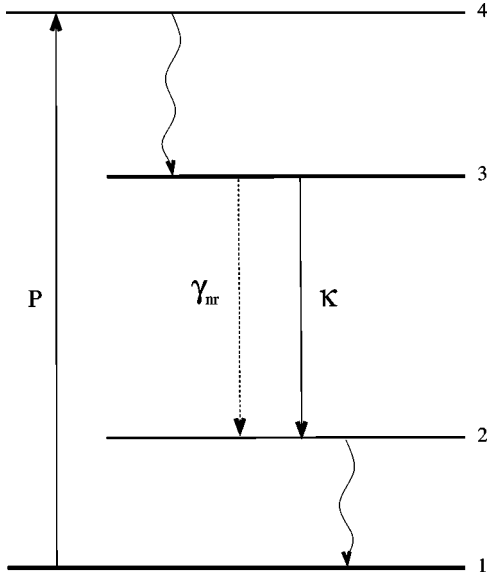


FIG. 1. Laser scheme for random laser. The transition 1→4 represents the pumping process, 3→2 (continuous line) corresponds to laser emission, the dashed line represents the relaxation process, and the wiggly arrows represent the rapid nonradiative decay processes.

Here, the pumping rate  $\mathcal{P}(\mathbf{r})$  is in units of spontaneous emission rate of the laser transition, and  $I_{sat}$  is the saturation intensity [24]. In what follows, we will make use of a simple mean-field theory, in which  $|E(\mathbf{r})|^2$  is replaced by  $\langle |E(\mathbf{r})|^2 \rangle_{ens}$ . In a homogeneous medium with a homogeneous pumping, this is independent of the position  $\mathbf{r}$ .

In a multiple-scattering medium, the propagation direction of light is continuously changed. In this case, one defines the transport mean free path  $l^*$  as the average distance the light travels in the random medium before its direction is randomized. For length scales larger than the transport mean free path, the phase correlation of waves can be ignored, and the wave equation (2.1) describing light transport in the random medium is replaced by a diffusion equation for the wave field intensity, as we will show below.

The coherence properties of the electromagnetic field are described by the Wigner coherence function, which represents the wave analogous of the specific intensity in radiative transfer theory. The specific intensity  $I_{spec}(\mathbf{R}, \mathbf{k})$  describes the number of photons in the vicinity of the point  $\mathbf{R}$ , traveling in the direction  $\hat{\mathbf{k}}$ . The uncertainty principle places a fundamental limit of how accurately both  $\mathbf{R}$  and  $\mathbf{k}$  can be simultaneously defined and this requires that we interpret  $\mathbf{R}$  and  $\mathbf{k}$  as “coarse-grained” variables. In contrast, the Wigner function is defined as the Fourier transform of the electric field autocorrelation function,

$$I(\mathbf{R}, T; \mathbf{k}, \omega) \equiv \int d\mathbf{r} dt e^{i\mathbf{k} \cdot \mathbf{r}} e^{-i\omega t} \langle E^*(\mathbf{R} + \mathbf{r}/2; T + t/2) \times E(\mathbf{R} - \mathbf{r}/2; T - t/2) \rangle_{ens}. \quad (2.6)$$

Here,  $E(\mathbf{r}; t)$  is the complex electric-field amplitude of the propagating radiation field. We note that the Wigner function

$I(\mathbf{R}, T; \mathbf{k}, \omega)$  defined in Eq. (2.6) is not necessarily positive definite and differs from the specific light intensity of radiative transfer theory, which is always positive definite. However, it can be demonstrated [25] that a suitable coarse graining of the Wigner distribution leads to a positive distribution which can be identified with the specific light intensity.

Consider an extended source (corresponding, in this case, to spontaneous emission of the excited atoms) in the vicinity of point  $\mathbf{R}'$  containing the points  $\mathbf{r}'_1$  and  $\mathbf{r}'_2$  [ $\mathbf{R}' \equiv (\mathbf{r}'_1 + \mathbf{r}'_2)/2$ ], and at time  $T' \equiv (t'_1 + t'_2)/2$ . The electric field generated by the source at point  $\mathbf{r}'$  and time  $t'$  is denoted by  $E_0(\mathbf{r}'; t')$ . The resulting field is measured by an extended detector in the vicinity of point  $\mathbf{R} \equiv (\mathbf{r}_1 + \mathbf{r}_2)/2$  and at time  $T \equiv (t_1 + t_2)/2$ . The resulting field autocorrelation function is given by

$$\begin{aligned} & \langle E^*(\mathbf{r}_1; t_1) E(\mathbf{r}_2; t_2) \rangle_{ens} \\ &= \frac{\omega^4}{c^4} \int_{\mathbf{r}'_1, \mathbf{r}'_2, t'_1, t'_2} \langle G^+(\mathbf{r}_1, \mathbf{r}'_1; t_1, t'_1) G^-(\mathbf{r}_2, \mathbf{r}'_2; t_2, t'_2) \rangle_{ens} \\ & \quad \times E_0(\mathbf{r}'_1; t'_1) E_0(\mathbf{r}'_2; t'_2). \end{aligned} \quad (2.7)$$

Here, we use the notation  $\int d\mathbf{r} \equiv \int_{\mathbf{r}}$ ,  $\int dt \equiv \int_t$ ,  $\int d\mathbf{k}/(2\pi)^3 \equiv \int_{\mathbf{k}}$ , and  $\int d\omega/2\pi \equiv \int_{\omega}$ . The Green's functions  $G^\pm(\mathbf{r}, \mathbf{r}'; t, t')$  in Eq. (2.7) are the advanced (with respect to  $t=0$ ) and retarded solutions of the wave equation

$$\left[ \nabla_{\mathbf{r}}^2 - \frac{\epsilon(\mathbf{r})}{c^2} \frac{\partial^2}{\partial t^2} \right] G(\mathbf{r}, \mathbf{r}'; t, t') = \delta(\mathbf{r} - \mathbf{r}') \delta(t - t'). \quad (2.8)$$

In a uniform medium, the advanced and retarded Green's functions correspond to the outgoing (+) and the incoming (−) waves associated with a point source. Since  $\epsilon(\mathbf{r})$  is assumed to be time independent, it follows that  $G^\pm$  depend only on the difference between its two time arguments. The corresponding ensemble-averaged Green's functions  $\langle G^\pm \rangle_{ens} \equiv G_{ens}^\pm$  describe an “effective” homogeneous medium. It follows that  $G_{ens}^\pm(\mathbf{r}, \mathbf{r}'; t, t') = G_{ens}^\pm(\mathbf{r} - \mathbf{r}'; t - t')$ .

It follows from Eqs. (2.6) and (2.7) that the Wigner function can be expressed as

$$I(\mathbf{R}, T; \mathbf{k}, \omega) = \int_{\mathbf{R}', T', \mathbf{k}', \omega'} \Gamma(\mathbf{R} - \mathbf{R}', T - T'; \mathbf{k}, \mathbf{k}', \omega, \omega') \times I_0(\mathbf{R}', T'; \mathbf{k}', \omega'). \quad (2.9)$$

Here,  $I_0(\mathbf{R}', T'; \mathbf{k}', \omega')$  is the source field Wigner coherence function, and the transport kernel  $\Gamma(\mathbf{R} - \mathbf{R}', T - T'; \mathbf{k}, \mathbf{k}', \omega, \omega')$  is given by

$$\begin{aligned} \Gamma(\mathbf{R}-\mathbf{R}', T-T'; \mathbf{k}, \mathbf{k}', \omega, \omega') &\equiv \int_{\mathbf{r}, \mathbf{r}', t, t'} \exp[-i\mathbf{k} \cdot \mathbf{r} + i\mathbf{k}' \cdot \mathbf{r}'] \exp[i\omega t - i\omega' t'] \langle G_{ens}^+(\mathbf{R}+\mathbf{r}/2, \mathbf{R}'+\mathbf{r}'/2; T+t/2, T'+t'/2) \\ &\times G_{ens}^-(\mathbf{R}-\mathbf{r}/2, \mathbf{R}'-\mathbf{r}'/2; T-t/2, T'-t'/2) \rangle_{ens}. \end{aligned} \quad (2.10)$$

In the case of a random amplifying medium,  $I_0(\mathbf{R}', T'; \mathbf{k}', \omega')$  is proportional to the excited atomic population at position  $\mathbf{R}'$  and time  $T'$ . The total dielectric function

$$\epsilon(\mathbf{r}) \equiv \epsilon_1(\mathbf{r}) + 4\pi\chi(\mathbf{r}) \quad (2.11)$$

contains both the nonlinear, intensity-dependent complex part  $\chi$ , and the linear part  $\epsilon$ , with random spatial fluctuations. As a consequence, applying the usual perturbative multiple-scattering theory [23,25,26], with  $\epsilon(\mathbf{r}) - \epsilon_0$  as the perturbation, becomes cumbersome. In what follows, we simplify the problem by using a mean-field approximation, in which we assume a nearly homogeneous population inversion. More precisely, we assume that the spatial variations in  $\mathcal{P}(\mathbf{r})$  occur slowly over length scales much longer than the transport mean free path. In this case, we can replace  $|E(\mathbf{r})|^2$  in Eq. (2.5) by a corresponding ‘‘coarse-grained’’ average value  $I_{avg} = \langle |E(\mathbf{r})|^2 \rangle_{coarse}$  where  $\langle \rangle_{coarse} \equiv (1/\Omega) \int d\mathbf{r}$ , and the sampling volume  $\Omega$  corresponds to the scale over which  $\mathcal{P}(\mathbf{r}) = \mathcal{P}$  is considered constant. This mean-field approximation for the nonlinear part of the wave equation allows us to perform perturbation theory [in the fluctuating linear part of the dielectric constant  $\epsilon_{fluct}(\mathbf{r})$ ] about the uniform part  $\bar{\epsilon}_0 \equiv \epsilon_0 + \chi_0 \mathcal{P} / (1 + I_{avg} / I_{sat})$ . The resulting perturbation theory is the standard multiple-scattering theory for an effective linear medium [26,25] with absorption and gain.

We define

$$\begin{aligned} \Gamma(\mathbf{Q}, \Omega; \mathbf{k}, \mathbf{k}', \omega) &\equiv \left(\frac{c}{\omega}\right)^4 \int_{\mathbf{R}, T} \exp(-i\mathbf{Q} \cdot \mathbf{R}) \\ &\times \exp(i\Omega T) \Gamma(\mathbf{R}, T; \mathbf{k}, \mathbf{k}', \omega). \end{aligned} \quad (2.12)$$

Neglecting interference of different radiative transfer paths, perturbation theory [23,27] leads to an integral equation (Bethe-Salpeter equation) for the transport kernel:

$$\begin{aligned} \Gamma(\mathbf{Q}, \Omega; \mathbf{k}, \mathbf{k}', \omega) &= G_{ens}^+(\mathbf{Q}/2 + \mathbf{k}, \Omega/2 + \omega) G_{ens}^-(\mathbf{Q}/2 - \mathbf{k}, \Omega/2 - \omega) \\ &\times \left[ \delta_{\mathbf{k}, \mathbf{k}'} + \int_{\mathbf{k}''} \tilde{B}(\mathbf{k} - \mathbf{k}'') \Gamma(\mathbf{Q}, \Omega; \mathbf{k}'', \mathbf{k}', \omega) \right]. \end{aligned} \quad (2.13)$$

Here,

$$G_{ens}^{\pm}(\mathbf{k}, \omega) \equiv \int_{\mathbf{r}, t} \exp(-i\mathbf{k} \cdot \mathbf{r}) \exp(i\omega t) G_{ens}^{\pm}(\mathbf{r}, t), \quad (2.14)$$

and  $\tilde{B}(\mathbf{k})$  is the Fourier transform of the complex dielectric autocorrelation function

$$B(\mathbf{r} - \mathbf{r}') \equiv \left(\frac{\omega}{c}\right)^4 \langle \epsilon_{fluct}(\mathbf{r}) \epsilon_{fluct}^*(\mathbf{r}') \rangle_{ens}. \quad (2.15)$$

This is a generalization of the ‘‘ladder approximation’’ for the summation of the scattering processes, well known in electronic transport [27,28], to include the effects of spatial correlations in the random potential and intensity-dependent (mean-field) imaginary part of the dielectric function. In the presence of absorption and gain, the mean-field single-photon Green’s functions in Eq. (2.13) are given by

$$G_{ens}^+(\mathbf{k}, \omega) = \frac{1}{\frac{\omega_+^2}{c^2} \bar{\epsilon}_0 - k^2 - \Sigma^+(\mathbf{k}, \omega)}, \quad (2.16a)$$

$$G_{ens}^-(\mathbf{k}, \omega) = \frac{1}{\frac{\omega_-^2}{c^2} \bar{\epsilon}_0^* - k^2 - \Sigma^-(\mathbf{k}, \omega)}, \quad (2.16b)$$

where  $\omega_{\pm} = \omega \pm i0^+$ ,  $\bar{\epsilon}_0$  is the complex homogeneous part of the dielectric function, and the self-energies

$$\Sigma^+(\mathbf{k}, \omega) = \int_{\mathbf{k}'} \tilde{B}'(\mathbf{k} - \mathbf{k}') G_{ens}^+(\mathbf{k}', \omega), \quad (2.17a)$$

$$\Sigma^-(\mathbf{k}, \omega) = \int_{\mathbf{k}'} \tilde{B}'^*(\mathbf{k} - \mathbf{k}') G_{ens}^-(\mathbf{k}', \omega) \quad (2.17b)$$

describe the effect of the scattering. Here,  $\tilde{B}'(\mathbf{k})$  is the Fourier transform of the dielectric autocorrelation function

$$B'(\mathbf{r} - \mathbf{r}') \equiv \left(\frac{\omega}{c}\right)^4 \langle \epsilon_{fluct}(\mathbf{r}) \epsilon_{fluct}(\mathbf{r}') \rangle_{ens}. \quad (2.18)$$

We note that, in the general case, when  $\epsilon_{fluct}(\mathbf{r})$  is a complex quantity, the dielectric function autocorrelation functions  $B$  and  $B'$  are distinct. For uniform absorption,  $B = B'$ . Using the expressions, Eq. (2.16), for the Green’s functions, Eq. (2.13) can be further transformed to the general form

$$\begin{aligned}
& -2\frac{\Omega}{c}\frac{\omega}{c}(\bar{\epsilon}_0 + \bar{\epsilon}_0^*)\Gamma(\mathbf{Q}, \Omega; \mathbf{k}, \mathbf{k}') - \frac{2}{c^2}\left(\frac{\Omega}{2}\right)^2(\bar{\epsilon}_0 - \bar{\epsilon}_0^*) \\
& \times \Gamma(\mathbf{Q}, \Omega; \mathbf{k}, \mathbf{k}') = -2\mathbf{k} \cdot \mathbf{Q}\Gamma(\mathbf{Q}, \Omega; \mathbf{k}, \mathbf{k}') \\
& + \mathcal{G}\Gamma(\mathbf{Q}, \Omega; \mathbf{k}, \mathbf{k}') + \Delta G_{ens}(\mathbf{Q}, \Omega, \mathbf{k}) \\
& \times \left[ \delta(\mathbf{k} - \mathbf{k}') + \int_{\mathbf{k}''} \tilde{B}(\mathbf{k} - \mathbf{k}'')\Gamma(\mathbf{Q}, \Omega; \mathbf{k}', \mathbf{k}'') \right. \\
& \left. - \Delta\Sigma(\mathbf{Q}, \Omega, \mathbf{k})\Gamma(\mathbf{Q}, \Omega; \mathbf{k}, \mathbf{k}') \right]. \quad (2.19)
\end{aligned}$$

Here and throughout the remainder of the paper, we omit the  $\omega$  dependence of the propagator  $\Gamma$  and specific intensity  $I$  for simplicity of notation. The gain coefficient  $\mathcal{G}$  in Eq. (2.19) corresponding to the presence of the amplifying medium is defined by

$$\mathcal{G} \equiv \frac{\omega_+^2}{c^2}\bar{\epsilon}_0 - \frac{\omega_-^2}{c^2}\bar{\epsilon}_0^* = 8\pi i \frac{\omega^2 \chi_0''}{c^2 V} \Delta N, \quad (2.20)$$

$$\begin{aligned}
\Delta G_{ens}(\mathbf{Q}, \Omega, \mathbf{k}) \equiv & G_{ens}^+(\mathbf{Q}/2 + \mathbf{k}, \Omega/2 + \omega) - G_{ens}^-(\mathbf{Q}/2 \\
& - \mathbf{k}, \Omega/2 - \omega), \quad (2.21)
\end{aligned}$$

and

$$\begin{aligned}
\Delta\Sigma(\mathbf{Q}, \Omega, \mathbf{k}) \equiv & \Sigma^+(\mathbf{Q}/2 + \mathbf{k}, \Omega/2 + \omega) \\
& - \Sigma^-(\mathbf{Q}/2 - \mathbf{k}, \Omega/2 - \omega). \quad (2.22)
\end{aligned}$$

Equation (2.19) describes wave propagation in a disordered active medium. It represents the generalization of the wave propagation equation for a passive random medium, studied in the literature [25].

The transport equation obeyed by the Wigner coherence function  $I(\mathbf{R}, T; \mathbf{k})$  is derived from Eq. (2.19) by performing an inverse Fourier transform with respect to  $\mathbf{Q}$  and  $\Omega$ , multiplying the resulting equation by  $I_0(\mathbf{R}', T'; \mathbf{k}')$ , and then integrating over  $\mathbf{R}'$ ,  $T'$ , and  $\mathbf{k}'$ . We obtain

$$\begin{aligned}
2\frac{\omega}{ic^2}\partial_T I(\mathbf{R}, T; \mathbf{k}) = & -\frac{2}{i}\mathbf{k} \cdot \nabla_{\mathbf{R}} I(\mathbf{R}, T; \mathbf{k}) + \mathcal{G}I(\mathbf{R}, T; \mathbf{k}) + \int_{\mathbf{R}', T'} \Delta G_{ens}(\mathbf{R} - \mathbf{R}', T - T'; \mathbf{k}) I_0(\mathbf{R}', T'; \mathbf{k}) \\
& + \int_{\mathbf{R}', T', \mathbf{k}'} \Delta G_{ens}(\mathbf{R}', T'; \mathbf{k}) \tilde{B}(\mathbf{k} - \mathbf{k}') I(\mathbf{R} - \mathbf{R}', T - T'; \mathbf{k}') \\
& - \int_{\mathbf{R}', T', \mathbf{k}'} \Delta\Sigma(\mathbf{R}', T'; \mathbf{k}) I(\mathbf{R} - \mathbf{R}', T - T'; \mathbf{k}'). \quad (2.23)
\end{aligned}$$

Here, we have considered the long time behavior, and used  $\Omega \ll \omega$ . Also, without loss of generality, we have set the real constant part of the dielectric function equal to 1. For a random dielectric medium with *homogeneous linear absorption*,  $B(\mathbf{r}) = B'(\mathbf{r})$  are real quantities, and one can replace the final term in Eq. (2.23) with

$$-\int_{\mathbf{R}', T', \mathbf{k}'} \Delta G_{ens}(\mathbf{R}', T'; \mathbf{k}') \tilde{B}(\mathbf{k} - \mathbf{k}') I(\mathbf{R} - \mathbf{R}', T - T'; \mathbf{k}'). \quad (2.24)$$

We note that the generalized transport equation (2.23) is formally analogous to the classical Boltzmann equation [29]. The conventional radiative transport equation can be obtained from Eq. (2.23) by *neglecting the nonlocal* spatial and temporal effects, arising from the phase correlations in the wave field [25]. Formally, this corresponds to neglecting the  $\mathbf{Q}$  and  $\Omega$  dependence of  $\Delta G_{ens}(\mathbf{Q}, \Omega, \mathbf{k})$ , i.e.,  $\Delta G_{ens}(\mathbf{Q}, \Omega, \mathbf{k}) \rightarrow \Delta G_{ens}(0, 0, \mathbf{k})$  [25]. Within this approximation, Eqs. (2.23) and (2.24) lead to

$$\begin{aligned}
& \partial_T I(\mathbf{R}, T; \mathbf{k}) \\
& = -c \hat{\mathbf{k}} \cdot \nabla I(\mathbf{R}, T; \mathbf{k}) + \frac{c^2 i}{2\omega} \mathcal{G} I(\mathbf{R}, T; \mathbf{k}) \\
& + \frac{c^2 i}{2\omega} \Delta G_{ens}(0, 0, \mathbf{k}) I_0(\mathbf{R}, T, \mathbf{k}) \\
& + \frac{c^2 i}{2\omega} \int_{\mathbf{k}'} \Delta G_{ens}(0, 0; \mathbf{k}) \tilde{B}(\mathbf{k} - \mathbf{k}') I(\mathbf{R}, T; \mathbf{k}') \\
& - \frac{c^2 i}{2\omega} \left( \int_{\mathbf{k}'} \Delta G_{ens}(0, 0, \mathbf{k}') B(\mathbf{k} - \mathbf{k}') \right) I(\mathbf{R}, T; \mathbf{k}). \quad (2.25)
\end{aligned}$$

We now make the identification between the coarse-grained Wigner coherence function  $I(\mathbf{R}, T, \mathbf{k})$  and mean number of photons,  $n_{\hat{\mathbf{k}}}(\mathbf{R}, T)$ , in the vicinity of a point  $\mathbf{R}$  and at time  $T$  and traveling in the direction of the wave vector  $\hat{\mathbf{k}}$ , and the notational change  $\mathbf{R} \leftrightarrow \mathbf{r}$  and  $T \leftrightarrow t$ . Using this interpretation, Eq. (2.25) leads to Boltzmann transport equation

[29] with gain, in which the source term is identified with spontaneous emission from the excited dye molecules:

$$\begin{aligned} \dot{\bar{n}}_{\hat{\mathbf{k}}}(\mathbf{r}) = & -c \hat{\mathbf{k}} \cdot \nabla \bar{n}_{\hat{\mathbf{k}}}(\mathbf{r}) + \sum_{\hat{\mathbf{k}}'} w_{\hat{\mathbf{k}}, \hat{\mathbf{k}}'} [\bar{n}_{\hat{\mathbf{k}}'}(\mathbf{r}) - \bar{n}_{\hat{\mathbf{k}}}(\mathbf{r})] \\ & + \kappa [\bar{n}_{\hat{\mathbf{k}}}(\mathbf{r}) + 1] \Delta \bar{N}(\mathbf{r}). \end{aligned} \quad (2.26)$$

Here, the scattering rates  $w_{\hat{\mathbf{k}}, \hat{\mathbf{k}}'}$  and  $w_{\hat{\mathbf{k}}', \hat{\mathbf{k}}}$  are related to the statistical properties of the dielectric background according to

$$w_{\hat{\mathbf{k}}, \hat{\mathbf{k}}'} = w_{\hat{\mathbf{k}}', \hat{\mathbf{k}}} = \frac{1}{2} i \frac{c^2}{\omega} \Delta G_{ens}(0, 0, |\mathbf{k}|) \tilde{B}(\mathbf{k} - \mathbf{k}'). \quad (2.27)$$

In our model, the scattering is assumed elastic and isotropic. As a result, the Green's functions only depend on the magnitude of the photon wave vector. The role of anisotropic scattering and nonlocal wave correlations will be the subject of a future study. In Eq. (2.26),  $\kappa = c \sigma_e / V \equiv 4 \pi \omega \chi_0'' / V$  is the radiative transition rate ( $\sigma_e$  is the stimulated emission cross section), and we make the identification  $(c^2/2\omega) i \Delta G_{ens}(0, 0, |\mathbf{k}|) I_0(\mathbf{r}, |\mathbf{k}|) \equiv \kappa \Delta \bar{N}(\mathbf{r})$  [note that  $\Delta G_{ens}(0, 0, |\mathbf{k}|) = 2i \text{Im} \Sigma^+(\mathbf{k})$  is purely imaginary]. In the transport equation (2.26), we have restored the possibility of slow spatial variations in the gain coefficient by identifying it with the position-dependent average atomic population inversion,  $\Delta \bar{N}(\mathbf{r})$ . This population inversion is obtained from the Einstein rate equation for the atomic system. In the four-level system described above (see Fig. 1) (we assume that the lower laser level is not populated due to rapid decay to lower levels), the average atomic population inversion is equal to the average atomic population  $N(\mathbf{r})$  in the excited state of the laser transition. This population obeys the equation

$$\dot{\bar{N}}(\mathbf{r}) = \mathcal{P}(\mathbf{r}) - \gamma_{nr} \bar{N}(\mathbf{r}) - \kappa [\bar{n}(\mathbf{r}) + 1] \bar{N}(\mathbf{r}). \quad (2.28)$$

Here, we have assumed isotropic atomic emission, and  $\bar{n}(\mathbf{r}) = \sum_{\hat{\mathbf{k}}} \bar{n}_{\hat{\mathbf{k}}}(\mathbf{r})$  is the average number of photons emitted in all directions.  $\gamma_{nr}$  in Eq. (2.28) is the rate of nonradiative decay of the laser transition.

For physical length scales larger than the transport mean free path, one can further make the *diffusion approximation* [29]. Formally, this consists in expanding the  $\hat{\mathbf{k}}$ -dependent functions in the transport equation (2.26) in spherical harmonics, and keeping only the first two terms of the expansion. This leads to the diffusion equation for the photons propagating in all directions,  $\bar{n}(\mathbf{r}) = \sum_{\hat{\mathbf{k}}} \bar{n}_{\hat{\mathbf{k}}}(\mathbf{r})$  (see Appendix A):

$$\dot{\bar{n}}(\mathbf{r}) = D \nabla_{\mathbf{r}}^2 \bar{n}(\mathbf{r}) + \kappa [\bar{n}(\mathbf{r}) + 1] \bar{N}(\mathbf{r}). \quad (2.29)$$

Here,  $D = cl^*/3$  is the classical diffusion coefficient ( $l^*$  is the transport mean free path for photons). Equation (2.29) describes the average properties of the random amplifying medium, and leads to a physical picture in which the entire medium, on average, is either below or above a lasing

threshold. This is in contrast with other studies [20], which claim that lasing comes from isolated and highly improbable, spatially localized, fluctuations away from the average. While such effects may occur in the real physical system, our mean-field theory description leading to a simple diffusion equation (2.29) neglects these isolated, fluctuation contributions to lasing. We also note that in the general case of a random, nonuniform, distribution of active material within the sample, the scattering rates may depend on the statistical distribution of both the dielectric background and gain medium. This appears formally as a dependence of the transport mean free path and associated diffusion coefficient on the absorption and gain [30].

### III. MASTER EQUATION FOR A RANDOM LASER

We now construct a probabilistic model for photon-number distribution function associated with Eqs. (2.26) and (2.29). In particular, we demonstrate that both these equations can be recaptured within a suitable factorization approximation for the master equation for the photon probability distribution. Moreover, we demonstrate that lasing occurs, on average, throughout the illuminated random medium when local pumping exceeds a specific threshold. The master equation describes the coherence properties of the emitted light below and above threshold. This is inferred from the degree of second-order coherence  $g^{(2)}(0)$  of the local photon distribution. Our model predicts that light emission above threshold not only exhibits a laserlike input-output intensity characteristic, but that the emission exhibits coherence properties similar to a traditional laser.

#### A. Master equation for the radiative transfer model with gain

We partition the sample into a collection of hypothetical cubic cells of side length  $l^*$  centered on the points of a cubic lattice with lattice constant  $a = l^*$ . These cells exchange photons with the neighboring cells, and the number of photons within each cell fluctuates in time due to atomic emission and absorption events. Each cell is labeled by a coarse-grained position vector  $\mathbf{r}$ . Assuming that  $l^* \gg \lambda$ , it is possible to simultaneously associate this approximate position  $\mathbf{r}$  and arbitrary wave vector  $\mathbf{k}$  with photons in the medium. Each cell labeled by  $\mathbf{r}$  is characterized by the joint distribution function  $P_{\mathbf{r}}^{\dots, n_{\hat{\mathbf{k}}}, \dots, N}$  describing the probability of having a state with  $n_{\hat{\mathbf{k}}}$  photons of wave vector  $(\omega/c)\hat{\mathbf{k}}$  and  $N$  atoms in the excited state.  $P_{\mathbf{r}}^{\dots, n_{\hat{\mathbf{k}}}, \dots, N}$  changes with time due to absorption and emission of photons by atoms within the cell, nonradiative decay of the excited atoms, populating the excited state of the laser transitions by a pumping mechanism, as well as transport of photons to and from neighboring cells. Here, we assume that the ground state of the laser transition is not populated, and neglect reabsorption of the emitted photons. As in a conventional laser master equation description, the rate at which photons are added to the cell by radiative emission when  $n_{\hat{\mathbf{k}}}$  photons propagating in the direction  $\hat{\mathbf{k}}$  are already present in the cell is given by  $\kappa(n_{\hat{\mathbf{k}}} + 1)NP_{\mathbf{r}}^{\dots, n_{\hat{\mathbf{k}}}, \dots, N}$ , where  $\kappa$  is the single-atom spontaneous

emission rate. This leads to a state with  $(n_{\hat{\mathbf{k}}}+1)$  photons propagating in the direction  $\hat{\mathbf{k}}$  and a corresponding decay of  $P_{\mathbf{r}}^{\dots n_{\hat{\mathbf{k}}}, \dots N}$  with time. The factor of  $(n_{\hat{\mathbf{k}}}+1)$  in the overall emission rate is the usual enhancement factor when  $n_{\hat{\mathbf{k}}}+1$  indistinguishable bosons appear in the final state [31]. On the other hand,  $P_{\mathbf{r}}^{\dots n_{\hat{\mathbf{k}}}, \dots N}$  can increase with time if there are initially  $(n_{\hat{\mathbf{k}}}-1)$  photons of wave vector  $\mathbf{k}$  in the background and  $N+1$  excited atoms, and a single photon is emitted by one of  $N+1$  atoms. The rate of increase of  $P_{\mathbf{r}}^{\dots n_{\hat{\mathbf{k}}}, \dots N}$  in this case is given by  $\kappa n_{\hat{\mathbf{k}}}(N+1)P_{\mathbf{r}}^{\dots n_{\hat{\mathbf{k}}}-1, \dots N+1}$ . This must then be summed over all possible choices  $\hat{\mathbf{k}}$  of the photon propagation directions.

Similarly, the nonradiative relaxation process of the atomic system will cause a decay of  $P_{\mathbf{r}}^{\dots n_{\hat{\mathbf{k}}}, \dots N}$  at a rate  $\gamma_{nr}N P_{\mathbf{r}}^{\dots n_{\hat{\mathbf{k}}}, \dots N}$ , if there are initial  $N$  atoms in the excited state and one of them nonradiatively decays to the laser ground state, and an increase of  $P_{\mathbf{r}}^{\dots n_{\hat{\mathbf{k}}}, \dots N}$ , if there are initially  $N+1$  excited atoms in the cell. The rate of this increase is  $(N+1)P_{\mathbf{r}}^{\dots n_{\hat{\mathbf{k}}}, \dots N+1}$ . On the other hand, the number of atoms in the excited state in the cell increases as a result of the pumping process, at the pumping rate  $\mathcal{P}(\mathbf{r})$ . This, in turn, leads to a decay of  $P_{\mathbf{r}}^{\dots n_{\hat{\mathbf{k}}}, \dots N}$ , at a rate  $\mathcal{P}(\mathbf{r})P_{\mathbf{r}}^{\dots n_{\hat{\mathbf{k}}}, \dots N}$ , if there are initially  $N$  atoms in the excited state, and to an increase, at a rate of  $\mathcal{P}(\mathbf{r})P_{\mathbf{r}}^{\dots n_{\hat{\mathbf{k}}}, \dots N-1}$ , if there are initially  $N-1$  atoms in the excited state.

The new dynamics of the photon probability distribution in a random medium arise from the inflow and outflow of photons from a given cell. In a simple model of isotropic random scattering, the photon of wave vector  $(\omega/c)(\hat{\mathbf{k}})$  travels ballistically in the direction  $\hat{\mathbf{k}}$  at the speed of light,  $c$ , over the length  $l^*$  after which its direction is randomized by scattering into a neighboring cell. The rate for this process is  $w = c/l^*$ . If there are initially  $n_{\hat{\mathbf{k}}}$  photons in the state  $\hat{\mathbf{k}}$  in the cell at  $\mathbf{r}$ , then the outflow of a photon would cause decay of  $P_{\mathbf{r}}^{\dots n_{\hat{\mathbf{k}}}, \dots N}$ . Since each of the  $n_{\hat{\mathbf{k}}}$  photons is leaving the cavity at the rate  $w$ , the overall decay rate of  $P_{\mathbf{r}}^{\dots n_{\hat{\mathbf{k}}}, \dots N}$  is given by  $-wn_{\hat{\mathbf{k}}}P_{\mathbf{r}}^{\dots n_{\hat{\mathbf{k}}}, \dots N}$ . On the other hand, if there are initially  $(n_{\hat{\mathbf{k}}}+1)$  photons in the cell, the outflow of a single photon will enhance  $P_{\mathbf{r}}^{\dots n_{\hat{\mathbf{k}}}, \dots N}$ . This enhancement could arise from any of the  $(n_{\hat{\mathbf{k}}}+1)$  photons initially present and the rate of increase of  $P_{\mathbf{r}}^{\dots n_{\hat{\mathbf{k}}}, \dots N}$  is given by  $w(n_{\hat{\mathbf{k}}}+1)P_{\mathbf{r}}^{\dots n_{\hat{\mathbf{k}}}+1, \dots N}$ .

In a conventional high-quality factor laser cavity, consisting of a pair of mirrors,  $w$  is the analog of the leakage rate of light from the laser. While a conventional laser has a large number of extraneous nonlasing modes, in the random laser, *all* modes can contribute equally on average to the overall lasing process. Light scattered in a random direction simply enters a neighboring cell which participates with comparable probability to the buildup of laser radiation. In other words, the rate  $\gamma_{las}$  of photons emitted by atoms into a lasing mode is equal to the total rate  $\kappa$  of photons spontaneously emitted.

The actual lasing efficiency of excited atoms, however, is diminished, in our model, by nonradiative relaxation described by a rate  $\gamma_{nr}$ , and we define an efficiency factor  $\beta \equiv \gamma_{las}/(\kappa + \gamma_{nr})$ . Moreover, the efficiency is severely offset by the fact that the cavity decay rate  $w$  is typically greater than the spontaneous emission rate [32]. In the language of conventional lasers, the cells of the random laser act as “bad cavities.”

The inflow of photons to the cell at  $\mathbf{r}$  from the neighboring cell at  $\mathbf{r}-\hat{\delta}_{\hat{\mathbf{k}}}$  containing  $n'_{\hat{\mathbf{k}}}$  photons occurs at a rate  $w n'_{\hat{\mathbf{k}}}$ . This rate must be weighted by the conditional probability  $P_{\mathbf{r}-\hat{\delta}_{\hat{\mathbf{k}}}}^{n'_{\hat{\mathbf{k}}}, n', N'}$  that there are in fact  $n'_{\hat{\mathbf{k}}}$  photons in the state  $\hat{\mathbf{k}}$ , when there are  $n'$  photons in all states and  $N'$  excited atoms in the cell at  $\mathbf{r}-\hat{\delta}_{\hat{\mathbf{k}}}$ . This leads to an increase in  $P_{\mathbf{r}}^{\dots n_{\hat{\mathbf{k}}}, \dots N}$ , provided that there are initially  $n_{\hat{\mathbf{k}}}-1$  photons in the cell at  $\mathbf{r}$ , and to a decrease in  $P_{\mathbf{r}}^{\dots n_{\hat{\mathbf{k}}}, \dots N}$  if there are initially  $n_{\hat{\mathbf{k}}}$  photons in the cell at  $\mathbf{r}$ . Overall, the rate of increase of  $P_{\mathbf{r}}^{\dots n_{\hat{\mathbf{k}}}, \dots N}$  due to the neighboring cell at  $\mathbf{r}-\hat{\delta}_{\hat{\mathbf{k}}}$  is given by  $\sum_{n'_{\hat{\mathbf{k}}}, n', N'} n'_{\hat{\mathbf{k}}} w P_{\mathbf{r}-\hat{\delta}_{\hat{\mathbf{k}}}}^{n'_{\hat{\mathbf{k}}}, n', N'} (P_{\mathbf{r}}^{\dots n_{\hat{\mathbf{k}}}-1, \dots N} - P_{\mathbf{r}}^{\dots n_{\hat{\mathbf{k}}}, \dots N})$ , summed over all possible choices  $\hat{\mathbf{k}}$  of the photon propagation directions. Here,  $\hat{\delta}_{\hat{\mathbf{k}}} = l^* \hat{\mathbf{k}}$ , and the conditional probability  $P_{\mathbf{r}}^{n_{\hat{\mathbf{k}}}, n, N}$  is defined from  $P_{\mathbf{r}}^{\dots n_{\hat{\mathbf{k}}}, \dots n_{\hat{\mathbf{k}}}', \dots N}$  as a sum (denoted by  $\{n_{\hat{\mathbf{k}}}'\}$ ) over all states  $\{\dots, n_{\hat{\mathbf{k}}}, \dots, n_{\hat{\mathbf{k}}}', \dots\}$  with fixed value of  $n_{\hat{\mathbf{k}}}$ , such that  $\sum_{\hat{\mathbf{k}}} n_{\hat{\mathbf{k}}} = n$ :

$$P_{\mathbf{r}}^{n_{\hat{\mathbf{k}}}, n, N} = \sum_{\{n_{\hat{\mathbf{k}}}'\}_{\hat{\mathbf{k}}' \neq \hat{\mathbf{k}}}} P_{\mathbf{r}}^{\dots n_{\hat{\mathbf{k}}}, \dots n_{\hat{\mathbf{k}}}', \dots N}. \quad (3.1)$$

Finally, the number of photons in the state  $\hat{\mathbf{k}}$  may vary due to the change of the direction of propagation of the photon, caused by scattering. The scattering of photons from state  $\hat{\mathbf{k}}$  containing  $n_{\hat{\mathbf{k}}}$  photons to state  $\hat{\mathbf{k}}'$  occurs at a rate  $w_{\hat{\mathbf{k}}\hat{\mathbf{k}}'} n_{\hat{\mathbf{k}}}$ , since all  $n_{\hat{\mathbf{k}}}$  photons may scatter at a rate  $w_{\hat{\mathbf{k}}\hat{\mathbf{k}}}'$ . This process results in the transfer of a photon from state  $\hat{\mathbf{k}}$  to state  $\hat{\mathbf{k}}'$ , and leads to a decay of  $P_{\mathbf{r}}^{\dots n_{\hat{\mathbf{k}}}, \dots N}$  at a rate  $w_{\hat{\mathbf{k}}\hat{\mathbf{k}}}' n_{\hat{\mathbf{k}}} P_{\mathbf{r}}^{\dots n_{\hat{\mathbf{k}}}, \dots n_{\hat{\mathbf{k}}}', \dots N}$ . On the other hand,  $P_{\mathbf{r}}^{\dots n_{\hat{\mathbf{k}}}, \dots N}$  increases in time, if there are initially  $n_{\hat{\mathbf{k}}}+1$  photons in state  $\hat{\mathbf{k}}$ , and one of them is scattered to state  $\hat{\mathbf{k}}'$ , provided that there are  $n_{\hat{\mathbf{k}}}'-1$  photons in state  $\hat{\mathbf{k}}'$ . The corresponding rate of increase of  $P_{\mathbf{r}}^{\dots n_{\hat{\mathbf{k}}}, \dots N}$  in this case is  $w_{\hat{\mathbf{k}}\hat{\mathbf{k}}}' n_{\hat{\mathbf{k}}} P_{\mathbf{r}}^{\dots n_{\hat{\mathbf{k}}}+1, \dots, n_{\hat{\mathbf{k}}}'-1, \dots N}$ . This must then be summed over all possible choices of photon propagation directions  $\hat{\mathbf{k}}$  and  $\hat{\mathbf{k}}'$ . We note that we neglect here the nonlocal wave correlations which could in principle arise in Eq. (2.23). In the case of very strong scattering such that  $l^* \approx \lambda$  (the vacuum wavelength of photons), the rate of change of  $I(\mathbf{R}, \mathbf{k})$  is influenced by  $I(\mathbf{R}', \mathbf{k}')$  even for  $|\mathbf{R}-\mathbf{R}'| \geq l^*$ . Moreover, in the incipient photon localization regime [33], strong wave-interference and correlation effects become important on scales  $|\mathbf{R}-\mathbf{R}'| \geq l^*$ . In this case, even the “ladder

approximation" [23] leading to Eq. (2.23) becomes inadequate. However, for present considerations we assume that  $l^* \gg \lambda$ . Consequently the scattering process does not affect the total number of photons propagating in all directions in a

given cell, nor is the photon distribution in a given cell influenced nonlocally by neighboring cells.

Putting all the above processes together, we arrive at the master equation

$$\begin{aligned} \dot{P}_{\mathbf{r}}^{\dots, n_{\hat{\mathbf{k}}}, \dots, N} = & -\kappa \sum_{\hat{\mathbf{k}}} [(n_{\hat{\mathbf{k}}}+1)NP_{\mathbf{r}}^{\dots, n_{\hat{\mathbf{k}}}, \dots, N} - n_{\hat{\mathbf{k}}}(N+1)P_{\mathbf{r}}^{\dots, n_{\hat{\mathbf{k}}-1}, \dots, N+1}] \\ & - \gamma_{nr}[NP_{\mathbf{r}}^{\dots, n_{\hat{\mathbf{k}}}, \dots, N} - (N+1)P_{\mathbf{r}}^{\dots, n_{\hat{\mathbf{k}}}, \dots, N+1}] + \mathcal{P}(\mathbf{r})[P_{\mathbf{r}}^{\dots, n_{\hat{\mathbf{k}}}, \dots, N-1} - P_{\mathbf{r}}^{\dots, n_{\hat{\mathbf{k}}}, \dots, N}] \\ & + w \left[ - \sum_{\hat{\mathbf{k}}} n_{\hat{\mathbf{k}}} P_{\mathbf{r}}^{\dots, n_{\hat{\mathbf{k}}}, \dots, N} + \sum_{\hat{\mathbf{k}}} (n_{\hat{\mathbf{k}}}+1) P_{\mathbf{r}}^{\dots, n_{\hat{\mathbf{k}}+1}, \dots, N} \right] + w \sum_{\hat{\mathbf{k}}} \sum_{n'_{\hat{\mathbf{k}}}, n', N'} n'_{\hat{\mathbf{k}}} P_{\mathbf{r}-\hat{\delta}_{\hat{\mathbf{k}}}}^{n'_{\hat{\mathbf{k}}}, n', N'} \\ & \times [P_{\mathbf{r}}^{\dots, n_{\hat{\mathbf{k}}-1}, \dots, N} - P_{\mathbf{r}}^{\dots, n_{\hat{\mathbf{k}}}, \dots, N}] + \sum_{\hat{\mathbf{k}}, \hat{\mathbf{k}}'} w_{\hat{\mathbf{k}}\hat{\mathbf{k}}'} [(n_{\hat{\mathbf{k}}}+1)P_{\mathbf{r}}^{\dots, n_{\hat{\mathbf{k}}+1}, \dots, n_{\hat{\mathbf{k}}'-1}, \dots, N} - n_{\hat{\mathbf{k}}}P_{\mathbf{r}}^{\dots, n_{\hat{\mathbf{k}}}, \dots, n_{\hat{\mathbf{k}}'}, \dots, N}]. \end{aligned} \quad (3.2)$$

In writing the master equation (3.2), we have used the weak scattering ( $l^* \gg \lambda$ ) assumption that different cells are uncorrelated. This assumption is needed to factorize the joint probabilities involving photons in neighboring cells into products of probabilities involving individual cells. Such factorization has been made in terms describing the inflow of photons. Thus, each cell can be regarded as an independent laser mode, in which the nonlinearity (saturation effects) may stabilize the total intensity of the radiation above threshold.

Summing over all states with fixed value of  $n_{\hat{\mathbf{k}}}$  such that  $\sum_{\hat{\mathbf{k}}} n_{\hat{\mathbf{k}}} = n$  in master equation (3.2) yields the master equation for the conditional probability  $P_{\mathbf{r}}^{n_{\hat{\mathbf{k}}}, n, N}$ :

$$\begin{aligned} \dot{P}_{\mathbf{r}}^{n_{\hat{\mathbf{k}}}, n, N} = & -\kappa \{ N(n+1)P_{\mathbf{r}}^{n_{\hat{\mathbf{k}}}, n, N} - (N+1)[n_{\hat{\mathbf{k}}}P_{\mathbf{r}}^{n_{\hat{\mathbf{k}}-1}, n-1, N+1} + (n-n_{\hat{\mathbf{k}}}-1)P_{\mathbf{r}}^{n_{\hat{\mathbf{k}}}, n-1, N+1}] \} - \gamma_{nr}[NP_{\mathbf{r}}^{n_{\hat{\mathbf{k}}}, n, N} - (N+1)P_{\mathbf{r}}^{n_{\hat{\mathbf{k}}}, n, N+1}] \\ & + \mathcal{P}(\mathbf{r})[P_{\mathbf{r}}^{n_{\hat{\mathbf{k}}}, n, N-1} - P_{\mathbf{r}}^{n_{\hat{\mathbf{k}}}, n, N}] + w[-nP_{\mathbf{r}}^{n_{\hat{\mathbf{k}}}, n, N} + (n_{\hat{\mathbf{k}}}+1)P_{\mathbf{r}}^{n_{\hat{\mathbf{k}}+1}, n+1, N} + (n+1-n_{\hat{\mathbf{k}}})P_{\mathbf{r}}^{n_{\hat{\mathbf{k}}}, n+1, N}] \\ & + w \left[ \bar{n}_{\hat{\mathbf{k}}}(\mathbf{r}-\mathbf{a}_{\hat{\mathbf{k}}})P_{\mathbf{r}}^{n_{\hat{\mathbf{k}}-1}, n-1, N} + \left( \sum_{\hat{\mathbf{k}}' \neq \hat{\mathbf{k}}} \bar{n}_{\hat{\mathbf{k}}'}(\mathbf{r}-\hat{\delta}_{\hat{\mathbf{k}}'}) \right) P_{\mathbf{r}}^{n_{\hat{\mathbf{k}}}, n-1, N} - \left( \sum_{\hat{\mathbf{k}}'} \bar{n}_{\hat{\mathbf{k}}'}(\mathbf{r}-\hat{\delta}_{\hat{\mathbf{k}}'}) \right) P_{\mathbf{r}}^{n_{\hat{\mathbf{k}}}, n, N} \right] \\ & + \sum_{\hat{\mathbf{k}}' \neq \hat{\mathbf{k}}} w_{\hat{\mathbf{k}}\hat{\mathbf{k}}'} [(n_{\hat{\mathbf{k}}}+1)P_{\mathbf{r}}^{n_{\hat{\mathbf{k}}+1}, n, N} - n_{\hat{\mathbf{k}}}P_{\mathbf{r}}^{n_{\hat{\mathbf{k}}}, n, N} + n_{\hat{\mathbf{k}}'}(P_{\mathbf{r}}^{n_{\hat{\mathbf{k}}-1}, n, N} - P_{\mathbf{r}}^{n_{\hat{\mathbf{k}}}, n, N})]. \end{aligned} \quad (3.3)$$

Here, we have used the expression  $\bar{n}_{\hat{\mathbf{k}}}(\mathbf{r}-\hat{\delta}_{\hat{\mathbf{k}}}) = \sum_{n'_{\hat{\mathbf{k}}}, n', N'} n'_{\hat{\mathbf{k}}} P_{\mathbf{r}-\hat{\delta}_{\hat{\mathbf{k}}}}^{n'_{\hat{\mathbf{k}}}, n', N'}$  for the average number of photons propagating in the  $\hat{\mathbf{k}}$  direction in the cell at  $\mathbf{r}-\hat{\delta}_{\hat{\mathbf{k}}}$ .

It is demonstrated in Appendix B that Eq. (3.3) reproduces the transport equation (2.26) within mean-field approximation  $\sum_{n_{\hat{\mathbf{k}}}, n, N} n_{\hat{\mathbf{k}}} NP_{\mathbf{r}}^{n_{\hat{\mathbf{k}}}, n, N} \approx \bar{n}_{\hat{\mathbf{k}}}(\mathbf{r})\bar{N}(\mathbf{r})$ .

### B. Master equation for the diffusion model with gain

For each cell centered at  $\mathbf{r}$ , we define the photon probability distribution  $P_{\mathbf{r}}^{n, N}$  describing the probability that a total number of  $n$  photons are propagating in all  $\hat{\mathbf{k}}$  directions and  $N$  atoms are in their excited state,

$$P_{\mathbf{r}}^{n, N} = \sum_{n_{\hat{\mathbf{k}}}} P_{\mathbf{r}}^{n_{\hat{\mathbf{k}}}, n, N}. \quad (3.4)$$

By summing over  $n_{\hat{\mathbf{k}}}$  in Eq. (3.3), we derive the master equation for  $P_{\mathbf{r}}^{n, N}$ :

$$\begin{aligned} \dot{P}_{\mathbf{r}}^{n, N} = & -\kappa[(n+1)NP_{\mathbf{r}}^{n, N} - n(N+1)P_{\mathbf{r}}^{n-1, N+1}] \\ & - \gamma_{nr}[NP_{\mathbf{r}}^{n, N} - (N+1)P_{\mathbf{r}}^{n, N+1}] \\ & + \mathcal{P}(\mathbf{r})[P_{\mathbf{r}}^{n, N-1} - P_{\mathbf{r}}^{n, N}] \\ & + w[-nP_{\mathbf{r}}^{n, N} + (n+1)P_{\mathbf{r}}^{n+1, N}] \\ & + w[P_{\mathbf{r}}^{n-1, N} - P_{\mathbf{r}}^{n, N}] \sum_{\hat{\mathbf{k}}} \bar{n}_{\hat{\mathbf{k}}}(\mathbf{r}-\hat{\delta}_{\hat{\mathbf{k}}}). \end{aligned} \quad (3.5)$$

For length scales much larger than the transport mean free path, one can use the approximation

$$\bar{n}_{\hat{\mathbf{k}}}(\mathbf{r}-\hat{\delta}_{\hat{\mathbf{k}}}) \approx \bar{n}_{\hat{\mathbf{k}}}(\mathbf{r}) - \hat{\delta}_{\hat{\mathbf{k}}} \cdot \nabla_{\mathbf{r}} \bar{n}_{\hat{\mathbf{k}}}(\mathbf{r}). \quad (3.6)$$

Further, we employ the *diffusion approximation* (A2) for  $\bar{n}_{\hat{\mathbf{k}}}(\mathbf{r})$  to obtain

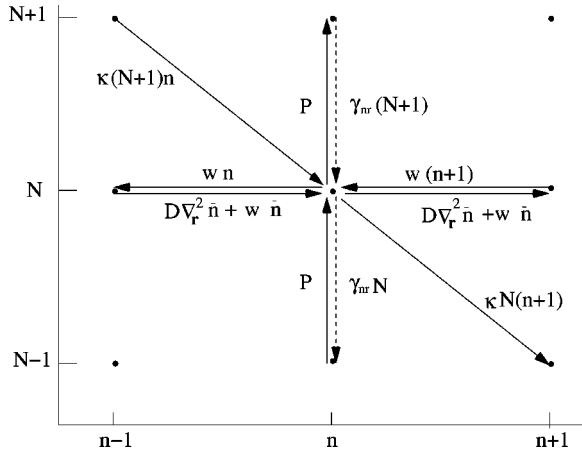


FIG. 2. Various transition processes described by the master equation of a random laser. The vertical arrows represent the photon-number conserving pumping (continuous line) and nonradiative relaxation (dashed line) processes. The horizontal arrows represent the excited atom-number conserving inflow (right arrows) and outflow (left arrows) of photons. The diagonal arrows correspond to spontaneous and stimulated emission, which increase the number of photons in a cell, and decrease the number of excited atoms.

$$\sum_{\mathbf{k}} \bar{n}_{\mathbf{k}}(\mathbf{r} - \delta\mathbf{k}) = \bar{n}(\mathbf{r}) - \frac{l^*}{c} \nabla_{\mathbf{r}} \cdot \mathbf{j}(\mathbf{r}) = \bar{n}(\mathbf{r}) + \frac{1}{w} D \nabla_{\mathbf{r}}^2 \bar{n}(\mathbf{r}). \quad (3.7)$$

For the second part of Eq. (3.7), we have used the steady-state current  $\mathbf{j}$  obtained from Eq. (A7), where we have neglected terms of the order  $l^*/l_g$  ( $l_g$  is the gain length defined in Appendix A). In Eq. (3.7),  $D = cl^*/3$  is the classical diffusion coefficient. This leads to the *diffusion master equation* for  $P_{\mathbf{r}}^{n,N}$ :

$$\begin{aligned} \dot{P}_{\mathbf{r}}^{n,N} = & -\kappa[(n+1)NP_{\mathbf{r}}^{n,N} - n(N+1)P_{\mathbf{r}}^{n-1,N+1}] \\ & -\gamma_{nr}[NP_{\mathbf{r}}^{n,N} - (N+1)P_{\mathbf{r}}^{n,N+1}] + \mathcal{P}_{\mathbf{r}}[P_{\mathbf{r}}^{n,N-1} - P_{\mathbf{r}}^{n,N}] \\ & + w[(n+1)P_{\mathbf{r}}^{n+1,N} - nP_{\mathbf{r}}^{n,N}] + [D \nabla_{\mathbf{r}}^2 \bar{n}(\mathbf{r}) + w\bar{n}(\mathbf{r})] \\ & \times [P_{\mathbf{r}}^{n-1,N} - P_{\mathbf{r}}^{n,N}]. \end{aligned} \quad (3.8)$$

Thus, we obtain a set of master equations for the laser modes at different positions within the sample. Each equation for a given  $\mathbf{r}$  (depicted schematically in Fig. 2) is similar, at any given position, to the master equation for a single-mode conventional laser [19]. In addition, the master equation for the random laser contains terms [the last group of terms in Eq. (3.8)] that correspond to the increasing of the photon number in a given cell due to the arrival of the photons through diffusion from the neighboring cells. We note that the rate of this process is always positive. The negative diffusion term  $D \nabla_{\mathbf{r}}^2 \bar{n}(\mathbf{r})$  can be expressed in steady-state limit from the diffusion equation (2.29) as  $-\kappa \bar{N}(\mathbf{r})[\bar{n}(\mathbf{r}) + 1]$ . Using then that  $\kappa = c\sigma_e/V$  (where  $\sigma_e$  is the emission cross section, and  $V$  is the volume of the sample), this term can be further expressed in terms of the absorption cross section  $\sigma_a$  absorption length  $l_a = (\sigma_a N_0/V)^{-1}$  (where  $N_0$

is the ground-state atomic population, assumed to be equal to the total atomic population), and normalized excited state population  $\bar{N}(\mathbf{r}) \equiv \bar{N}(\mathbf{r})/N_0$ , as  $-(\sigma_e/\sigma_a)(c/l_a)\bar{N}(\mathbf{r})[\bar{n}(\mathbf{r}) + 1] \approx -(c/l_a)\bar{n}(\mathbf{r})$ . On the other hand, the term  $w\bar{n}(\mathbf{r})$  is of the order of  $(c/l^*)\bar{n}(\mathbf{r})$ . This is greater than the absolute value of the diffusion term, for values of the transport mean free path and absorption length ( $l_a \gg l^*$ ), within the range of validity of a diffusion model.

The master equation (3.8) determines the equations of evolution for the average number of photons in the laser mode and excited atoms,  $\bar{n}(\mathbf{r}) = \sum_{n,N} n P_{\mathbf{r}}^{n,N}$  and  $\bar{N}(\mathbf{r}) = \sum_{n,N} N P_{\mathbf{r}}^{n,N}$ , respectively:

$$\dot{\bar{n}}(\mathbf{r}) = D \nabla_{\mathbf{r}}^2 \bar{n}(\mathbf{r}) + \overline{\kappa N(\mathbf{r})[n(\mathbf{r}) + 1]}, \quad (3.9a)$$

$$\dot{\bar{N}}(\mathbf{r}) = \mathcal{P}(\mathbf{r}) - \gamma_{nr} \bar{N}(\mathbf{r}) - \overline{\kappa N(\mathbf{r})[n(\mathbf{r}) + 1]}. \quad (3.9b)$$

Clearly, in the mean-field approximation  $\overline{N(\mathbf{r})n(\mathbf{r})} = \bar{N}(\mathbf{r})\bar{n}(\mathbf{r})$ , Eqs. (3.9a) and (3.9b) reproduce the diffusion-rate equations (2.28) and (2.29) used to describe the emission spectral and temporal properties of a random laser [11].

#### IV. STEADY-STATE PHOTON DISTRIBUTION FUNCTION

Laser photon statistics are obtained from the photon distribution function  $P_{\mathbf{r}}^n = \sum_N P_{\mathbf{r}}^{n,N}$  which describes the probability that  $n$  photons occupy the cell centered at  $\mathbf{r}$ . In order to obtain the master equation for  $P_{\mathbf{r}}^n$ , we sum over  $N$  in Eq. (3.8). The terms corresponding to pump and relaxation processes sum to zero, and we obtain

$$\begin{aligned} \dot{P}_{\mathbf{r}}^n = & -\{\kappa(n+1)\mathcal{N}(n,\mathbf{r})P_{\mathbf{r}}^n + [D \nabla_{\mathbf{r}}^2 \bar{n}(\mathbf{r}) + w\bar{n}(\mathbf{r})]P_{\mathbf{r}}^n \\ & - w(n+1)P_{\mathbf{r}}^{n+1}\} + \{\kappa n\mathcal{N}(n-1,\mathbf{r})P_{\mathbf{r}}^{n-1} \\ & + [D \nabla_{\mathbf{r}}^2 \bar{n}(\mathbf{r}) + w\bar{n}(\mathbf{r})]P_{\mathbf{r}}^{n-1} - wnP_{\mathbf{r}}^n\}, \end{aligned} \quad (4.1)$$

Here,  $\mathcal{N}(n,\mathbf{r}) \equiv \sum_N N P_{\mathbf{r}}^{n,N}/P_{\mathbf{r}}^n$  is the number of excited atoms in the cell centered at  $\mathbf{r}$  when precisely  $n$  photons occupy the cell.

For continuous wave pumping, we obtain that the steady state is maintained by the balancing of transitions between neighboring photon states. This corresponds to setting the terms in curly brackets in Eq. (4.1) to zero, individually:

$$[\kappa(n+1)\mathcal{N}(n,\mathbf{r}) + D \nabla_{\mathbf{r}}^2 \bar{n}(\mathbf{r}) + w\bar{n}(\mathbf{r})]P_{\mathbf{r}}^n = w(n+1)P_{\mathbf{r}}^{n+1}. \quad (4.2)$$

The factor by which the photon-number distribution functions corresponding to two neighboring photon states differ from each other,

$$f(n,\mathbf{r}) \equiv \frac{\kappa \mathcal{N}(n,\mathbf{r})}{w} + \frac{D \nabla_{\mathbf{r}}^2 \bar{n}(\mathbf{r}) + w\bar{n}(\mathbf{r})}{w(n+1)}, \quad (4.3)$$

is always positive. As argued in Sec. III, the second term in Eq. (4.3) is always positive.

The detailed balance equation for the random laser, Eq. (4.2), has the solution

$$P_{\mathbf{r}}^n = P_{\mathbf{r}}^0 \prod_{k=0}^{n-1} \left[ \frac{\kappa \mathcal{N}(k, \mathbf{r})}{w} + \frac{D \nabla_{\mathbf{r}}^2 \bar{n}(\mathbf{r}) + w \bar{n}(\mathbf{r})}{w(k+1)} \right]. \quad (4.4)$$

We note that calculating the photon distribution function  $P_{\mathbf{r}}^n$  requires knowledge of the mean number of photons,  $\bar{n}(\mathbf{r})$ , which, in turn, is determined by  $P_{\mathbf{r}}^n$ . The necessity of knowing the average photon number in order to determine the emission statistics is in our model a consequence of the assumption that optical modes in different cells are uncorrelated. By factorizing the probability distributions at different positions, we obtain that the probability of photon arrival into a spatial mode only depends on the average number of photons in the neighboring spatial modes. Here, we derive the statistics of the random laser by solving self-consistently the rate equations obtained from Eqs. (3.9a) and (3.9b) in the mean-field approximation together with Eq. (4.4).

The photon distribution function defined in Eq. (4.4) exhibits two types of behavior, depending on whether  $f(0, \mathbf{r})$  is less than unity or exceeds unity. In the former case,  $P_{\mathbf{r}}^n$  decreases with  $n$ . In the latter case,  $P_{\mathbf{r}}^n$  increases with  $n$  until it reaches a maximum and then decreases with further increasing of  $n$ . The transition between the two regimes determines the threshold for the crossover in the statistical behavior of laser radiation. This transition is defined by the condition  $f(0, \mathbf{r}) = 1$ , which takes the form

$$\kappa \mathcal{N}(0, \mathbf{r}) + D \nabla_{\mathbf{r}}^2 \bar{n}(\mathbf{r}) = w[1 - \bar{n}(\mathbf{r})]. \quad (4.5)$$

On the other hand, it is straightforward to show (see Appendix C) that the condition  $f(0, \mathbf{r}) = 1$  implies  $\bar{n}(\mathbf{r}) = 1$ . Consequently, the threshold condition (4.5) for the change in statistics becomes

$$\kappa \mathcal{N}(0, \mathbf{r}) + D \nabla_{\mathbf{r}}^2 \bar{n}(\mathbf{r}) = 0. \quad (4.6)$$

Equation (4.6) expresses the condition that the unsaturated gain  $\kappa \mathcal{N}(0, \mathbf{r})$  equals the diffusion ‘‘cavity loss’’  $-D \nabla_{\mathbf{r}}^2 \bar{n}(\mathbf{r})$ . This is the analog of the Schalow-Townes threshold condition for random-laser action. Therefore, in our model of a random laser, the laser oscillation threshold coincides with the photon statistics crossover point. This result is in good agreement with the experimental findings [9,10].

As discussed above, if the laser is operating above threshold, the photon distribution function has a peak at  $n = \bar{n}(\mathbf{r})$  defined by the condition

$$P_{\mathbf{r}}^{\bar{n}+1} = P_{\mathbf{r}}^{\bar{n}}. \quad (4.7)$$

This is equivalent to

$$\frac{1}{w} \{D \nabla_{\mathbf{r}}^2 \bar{n}(\mathbf{r}) + \kappa \mathcal{N}(\bar{n}, \mathbf{r})[\bar{n}(\mathbf{r}) + 1]\} = \bar{n}(\mathbf{r}) - \bar{n}(\mathbf{r}). \quad (4.8)$$

Here we have used that, above threshold,  $\bar{n}(\mathbf{r}) + 1 \approx \bar{n}(\mathbf{r})$ . The only positive solution  $\bar{n}$  of Eq. (4.8) is  $\bar{n}(\mathbf{r}) = \bar{n}(\mathbf{r})$ , where  $\bar{n}(\mathbf{r})$  is the mean-field solution of the steady-state rate-diffusion equation (3.9a). This shows that, similar to the case of a conventional laser [34], the average numbers of photons

given by the rate equation and the peak photon number in the master equation for a random laser are the same above threshold.

## V. STATISTICAL PROPERTIES OF THE EMITTED LASER LIGHT

The statistical properties and coherence of the emitted radiation can be studied using the Fano-Mandel parameter [35]  $F \equiv [\bar{n}^2 - \bar{n}^2 - \bar{n}]/\bar{n}$ , describing photon-number fluctuations. Here,  $\bar{n}^2(\mathbf{r}) = \sum_n n^2 P_{\mathbf{r}}^n$  and  $g^{(2)}(0) \equiv (\bar{n}^2 - \bar{n})/(\bar{n})^2 = F/\bar{n} + 1$  is the well-known degree of second-order coherence [36]. For chaotic (incoherent) light  $g^{(2)}(0) = 2$ , whereas for Poissonian (coherent) light  $g^{(2)}(0) = 1$ . For a laser operating well below threshold, in a weakly excited thermal state, as well as for a laser operating well above threshold, in a coherent state,  $F \rightarrow 0$ . In a conventional laser with  $\beta \approx 10^{-5}$ , the Fano parameter exhibits a sharp peak as a function of pump intensity at the lasing threshold [19]. The large fluctuations in the threshold region are indicative of a phase transition. As the spontaneous emission factor  $\beta$  increases, this peak becomes smaller and wider.

We obtain photon statistics and optical coherence defined by  $F$  at various positions  $\mathbf{r}$  within the random-laser sample by evaluating  $P_{\mathbf{r}}^n$ . To this end, Eq. (4.4) and the diffusion equation (2.29) are solved self-consistently. Here, we use the steady-state atomic excitation number,  $\mathcal{N}(n, \mathbf{r})$ , obtained from the rate equation for the atom number, similar to Eq. (2.28). In the presence of a stationary photon distribution  $P_{\mathbf{r}}^n$  (consistent with a four-level laser scheme described above), this takes the form [34]

$$\mathcal{N}(n, \mathbf{r}) = \frac{\mathcal{P}(\mathbf{r})}{[\gamma_{nr} + \kappa(n+1)]}. \quad (5.1)$$

We then calculate the average number of excited atoms as  $\bar{N}(\mathbf{r}) = \sum_n P_{\mathbf{r}}^n \mathcal{N}(n, \mathbf{r})$ . Equation (5.1) together with Eq. (4.4) and the mean-field factorization of Eq. (3.9a) provides a closed set of equations for  $P_{\mathbf{r}}^n$  and  $\bar{n}(\mathbf{r})$ . The expression (5.1) for the atomic excitation number corresponds to an ‘‘adiabatic elimination’’ of the atomic variables. We note that the typical ‘‘cavity decay rate’’  $w$  for a random laser is much faster than the atomic transition rates  $\kappa$ . For example, for a transport mean free path  $l^* = 100\lambda$ ,  $w$  corresponds to a picosecond time scale, while  $\kappa$  corresponds to a nanosecond time scale. As such, the adiabatic approximation is not rigorously justified. However, this leads to a much simpler analysis, which qualitatively agrees with the more complicated numerical analysis of the nonadiabatic atomic response. The difference between the results for the photon statistics obtained using a full master equation treatment, based on Eq. (3.8), and those obtained within the adiabatic approximation (Scully-Lamb theory) is illustrated for a few sets of parameters in Sec. VII.

For concreteness, we consider a slab in the  $xy$  plane, between the two planes  $z=0$  and  $z=L$ . We define  $z < 0$  as the left region and  $z > 0$  as the right region. A pumping beam is collimated perpendicular to  $z=0$  plane from the left. The

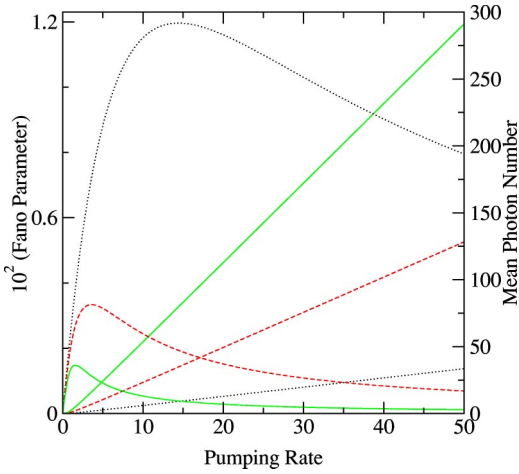


FIG. 3. Fano parameter and average photon number at different locations within the random laser sample, for a transport mean free path of  $10^{-4}$  cm and absorption length of  $1.5 \times 10^{-2}$  cm. The position within the sample is  $0.25l^*$  (dotted line),  $l^*$  (dashed line), and  $2.5l^*$  (continuous line), respectively, from the front of the sample. We set  $\beta=0.1$  and  $L=1$  cm in the calculations, and the pumping rate is in units of  $\Gamma \equiv \kappa + \gamma_{nr}$ .

light emitted from the sample is measured by a detector on the left [2]. This geometry is close to that of the cells used in some experiments [37].

In Fig. 3, we plot the Fano-Mandel parameter as a function of incident pumping rate, at different depths within the random-laser sample, for fixed scatterer density and gain concentration. As with a conventional laser, the Fano-Mandel parameter exhibits a fluctuation peak indicative of a transition from chaotic to coherent light. The magnitude of the fluctuation peak decreases deeper within the sample, due to attenuation of the local pumping intensity as it penetrates deeper into the sample. Deeper into the sample, the fluctuations also decrease more rapidly with the increasing of the pump above threshold. This suggests that the light emitted from deeper inside the sample, although weaker in intensity, is more coherent than that emitted from near the front face of the sample. These modes, however, have smaller contribution to the total laser radiation detected outside of the sample, as we show below.

The Fano-Mandel parameter as a function of incident pumping rate and different values of the scatterer density and gain concentration, at a given depth within the sample, is presented in Fig. 4. It is apparent that optical coherence, above threshold, is enhanced in samples with higher scatterer density and lower gain molecule concentration, within the range of parameters studied.

The output radiation (outside of the sample) is obtained as a weighted average of the contributions from different points within the sample [11]. In our model, different spatial modes are assumed uncorrelated. In this case, the Fano factor for the total output radiation is

$$F_{output} = \frac{\sum_i (\bar{n}_i^2 - \bar{n}_i^2 - \bar{n}_i)}{\sum_i \bar{n}_i} = \frac{\sum_i \bar{n}_i F_i}{\sum_i \bar{n}_i}, \quad (5.2)$$

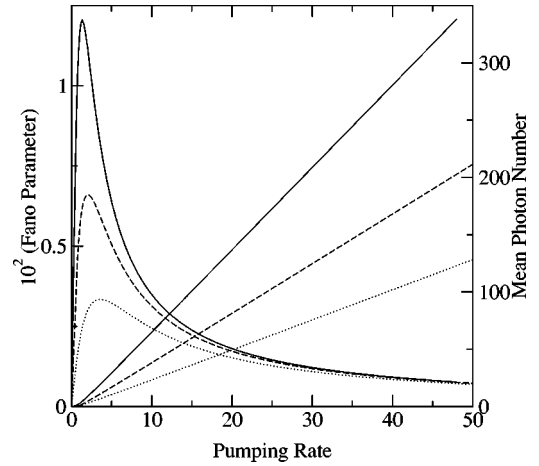


FIG. 4. Fano parameter and average photon number as a function of scaled pumping rate at the position  $z=l^*$  within the random-laser sample and for different values of the transport mean free path and absorption length:  $l^*=10^{-3}$  cm and  $l_a=1.5 \times 10^{-2}$  cm (continuous line),  $l^*=10^{-4}$  cm and  $l_a=1.5 \times 10^{-2}$  cm (dashed line), and  $l^*=10^{-3}$  cm and  $l_a=5.0 \times 10^{-3}$  cm (dotted line). The other sample parameters are the same as for Fig. 3.

where  $n_i$  and  $F_i$  are the photon number and the Fano factor for the  $i$ th cell within the sample, respectively. Generally, each cell  $i$  is defined by both the position  $z$  and the wave vector of the emerging photon,  $(\omega/c)\hat{\mathbf{k}}_f$ . The deeper the cell  $i$  is within the sample, the smaller the probability (weight factor) that photons from this cell will emerge from the sample without further scattering. More specifically, in Eq. (5.2),

$$\sum_i \dots \equiv \frac{1}{l^*} \sum_{z, \mathbf{k}} \exp\left(-\frac{z}{|\hat{\mathbf{k}}_f \cdot \hat{\mathbf{z}}| l^*}\right) \dots \quad (5.3)$$

Here,  $\exp(-z/|\hat{\mathbf{k}} \cdot \hat{\mathbf{z}}| l^*)$  represents the fraction of the radiation at  $z$  that emerges without being further scattered [38]. In our (diffusion) model, the wave-vector dependence of different physical quantities is not considered. After performing the wave-vector (angular) integration, the mode summation in continuum limit becomes

$$\sum_i \dots = \frac{1}{l^*} \int_0^L dz h(z) \dots \quad (5.4)$$

Here,  $h(z) = \rho(z) / \int_0^L dz \rho(z)$ , and  $\rho(z) = (1/4\pi) \int d\hat{\mathbf{k}}_f \exp[-z/(|\hat{\mathbf{k}}_f \cdot \hat{\mathbf{z}}| l^*)]$  is a function that decreases rapidly with the position within the sample. Clearly, only the radiation emitted within a few transport mean free paths from front face of the sample contributes significantly to the total output radiation. The Fano parameter for the total output radiation for various values of the scatterer density and gain concentration is presented in Fig. 5. Once again we observe a transition from chaotic to coherent light at specific pump threshold. We also find that optical coherence, above threshold, is enhanced in samples with shorter mean free path (stronger

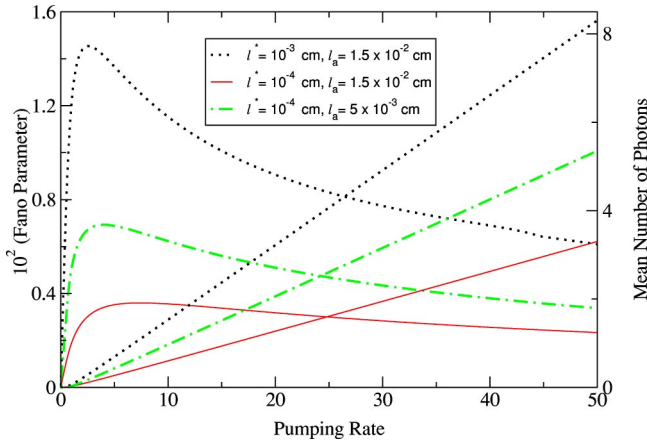


FIG. 5. Fano parameter and average photon number for the output radiation, for various scatterer and gain parameters. The other sample parameters are the same as for Fig. 3.

scattering) and lower gain molecule concentration, mirroring the behavior of the Fano parameter of individual cells within the sample.

## VI. INTERPRETATION OF NUMERICAL RESULTS

We now provide a qualitative interpretation of the results obtained in this paper. Suppose that the laser is operating above threshold. In this regime, we have shown above that the photon distribution function  $P_{\mathbf{r}}^n$  has a peak at the value of  $n = \bar{n}$ , equal to the mean number of photons. We further assume that for  $n$  close to  $\bar{n}$ ,  $P_{\mathbf{r}}^n$  can be written as (omitting the dependence on the spatial coordinate  $z$ ):

$$P^n = P^{\bar{n}} \exp\left[-\frac{(n - \bar{n})^2}{2\sigma^2}\right]. \quad (6.1)$$

On the other hand, from Eq. (4.4) we obtain

$$P^n = P^{\bar{n}} \left[ \prod_{n'=\bar{n}}^n f(n') \right]^{\pm 1}, \quad (6.2)$$

where  $\pm 1$  on the exponent correspond to  $n$  greater or smaller than  $\bar{n}$ , respectively.

Equations (6.1) and (6.2) lead to the equation for the variance  $\sigma$ :

$$-\frac{(n - \bar{n})^2}{2\sigma^2} = \pm \sum_{n'=\bar{n}}^n \ln[f(n')]. \quad (6.3)$$

Above threshold,  $\bar{n} \approx \bar{n} + 1$ . Since  $f(\bar{n}) = 1$ , it follows, for values of  $n$  close to  $\bar{n}$ ,

$$\ln[f(n')] \approx \pm (n' - \bar{n}) \left( \frac{1}{f(n')} \frac{df}{dn'} \right)_{n'=\bar{n}}. \quad (6.4)$$

Making use of Eqs. (4.3), (6.3), and (6.4), and the fact that  $w = c/l^*$ , we obtain

$$1 + F = \sigma^2 = \frac{\bar{n}}{1 - l^* N_0 \frac{\kappa \bar{N}}{[\gamma_{nr} + \kappa(\bar{n} + 1)]} \frac{\gamma_{nr}}{c}} > \bar{n} \quad (6.5)$$

(note that  $\sigma^2 = \bar{n}$  for a Poissonian distribution).

The results presented in Figs. 3 and 4 can now be easily explained using Eq. (6.5); namely, the amount of fluctuations in the emitted light decrease with the increasing of scatterer density (decreasing of  $l^*$ ), and with the decreasing of gain concentration ( $N_0$ ). Also, a sizable suppression of fluctuations is obtained for positions deeper into the sample, where  $\bar{N}$  decreases and  $\bar{n}$  increases.

In the mean-field analysis presented above, we have obtained an average diffusion coefficient with a constant value throughout the sample. More generally, the transport mean free path may vary randomly from region to region within the sample. This gives rise to additional fluctuations of the laser emission, related to the statistics of the diffusion coefficient. A description of such effects requires solving the diffusion equation and the equation for the photon distribution function (4.4) for an ensemble of systems characterized by a probability distribution of transport mean free paths. A detailed microscopic analysis of this issue is beyond the scope of this paper. Instead, we provide a qualitative discussion using Eq. (6.5) to illustrate how random spatial variations of the diffusion coefficient translate into fluctuations of the laser emission.

According to the expression (6.5), statistical fluctuations in  $l^*$  lead to corresponding fluctuations in  $F$ . The probability distribution for  $F$  is given by

$$\mathcal{P}_F(F) = \int dl^* \mathcal{P}_{l^*}(l^*) \delta(F - F(l^*)). \quad (6.6)$$

Here  $\mathcal{P}_{l^*}$  is the distribution of the transport mean free path over an ensemble of systems, and  $F(l^*)$  is given by Eq. (6.5). In order to facilitate an analytical investigation, we consider a regime where the laser is operating above threshold, but below the saturation regime, such that  $\beta \bar{n} \ll 1$ . For a random laser, we choose  $\beta = \kappa / (\kappa + \gamma_{nr})$ . In this case, the average excited state atomic population is given by  $\bar{N} = \mathcal{P} / [\gamma_{nr} + \kappa(\bar{n} + 1)] \approx \mathcal{P} / (\gamma_{nr} + \kappa)$  and we rewrite the denominator in Eq. (6.5) as  $1 - l^* \alpha$ , where

$$\alpha \equiv \frac{\mathcal{P}}{c} \frac{\gamma_{nr}}{\kappa} \beta^2. \quad (6.7)$$

Usually,  $l^* \alpha \ll 1$ . This enables an expansion of the denominator in Eq. (6.5), and the Fano parameter is approximated by

$$F \approx l^* \alpha. \quad (6.8)$$

If the statistical distribution  $\mathcal{P}_{l^*}$  of the transport mean free path is a Gaussian with mean  $\bar{l}^*$  and standard deviation  $\sigma_{l^*}$ , the distribution (6.6) of the Fano parameter is a Gaussian distribution with mean  $\alpha \bar{l}^*$  and standard deviation  $\alpha \sigma_{l^*}$ . We note that the more complex dependence of the Fano param-

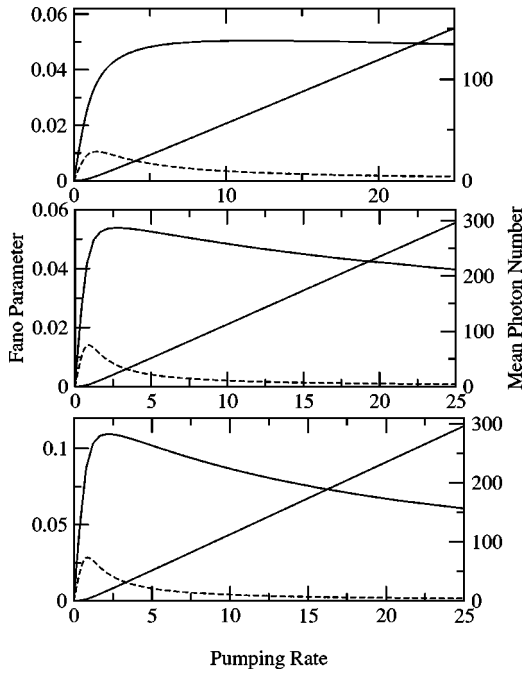


FIG. 6. Fano parameter and average photon number obtained from a solution of the truncated master equation (3.8) (continuous lines) and from the master equation (4.1) (dotted lines), respectively, at a position  $z=l^*$  within the sample, and for different values of the transport mean free path: (a)  $l^*=0.5$  cm, (b)  $l^*=1.0$  cm, and (c)  $l^*=2$  cm. We set  $l_a=15$  cm,  $L=10$  cm, and  $\beta=0.1$  in the calculations. The pumping rate is in units of  $\Gamma \equiv \kappa + \gamma_{nr}$ .

eter on transport mean free path, both directly (by the direct presence of  $l^*$  in the detailed balance equation (4.4) for the photon distribution function) and through the implicit dependence of the mean number of photons on the transport mean free path (generally, a power law [11]), will lead to a non-Gaussian distribution of the Fano parameter. Moreover, this distribution will be different for a laser operating below threshold as opposed to above threshold, because of the different dependence of the mean number of photons on the “cavity loss rate” ( $c/l^*$ ) in the two regimes [22].

## VII. NONADIABATIC ATOMIC RESPONSE

The previous analysis of photon statistics in the random laser is based on the Scully-Lamb [14] approach, where the atomic variables are adiabatically eliminated. As discussed above, an adiabatic elimination of the atomic variables is not rigorously justified for a random laser. This is particularly evident in strong scattering systems, where  $c/l^* \gg \kappa$ . We show here, by comparison, that it still recaptures the important qualitative features of the photon statistics of the emitted radiation. In order to examine the role of nonadiabatic atomic response of the atomic population to the local electromagnetic field, we investigate the laser statistics for a few sets of parameters. This is done using a full treatment, based on the master equation (3.8). The probability distribution function  $P_r^{n,N}$  is calculated by truncating the master equation (3.8) at some maximum values of  $n$  and  $N$ , which we denote

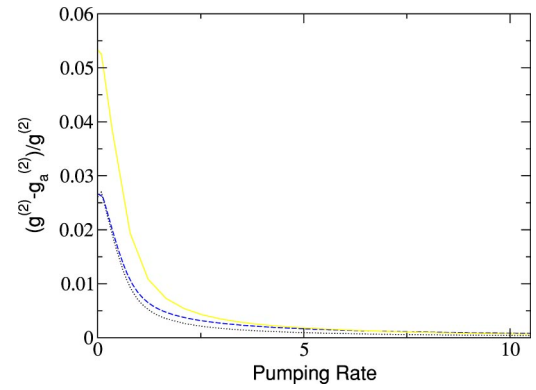


FIG. 7. The relative difference between the second-order correlation functions calculated using a full master equation treatment [ $g^{(2)}(0)$ ], and adiabatic elimination of atomic variables [ $g_a^{(2)}(0)$ ], at a position  $z=l^*$  within the sample, and for transport mean free paths of 0.5 cm (dashed line), 1 cm (dotted line), and 2 cm (continuous line). The other parameters are the same as for Fig. 6.

as  $n_{trunc}$  and  $N_{trunc}$ , respectively. The validity of the truncation is ensured by requiring that  $P_r^{n,N}$  does not change as  $n_{trunc}$  and  $N_{trunc}$  increase. This implies solving a system of  $(n_{trunc} + 1)(N_{trunc} + 1)$  coupled equations for  $P_r^{n,N}$  for all values  $0 \leq n \leq n_{trunc}$  and  $0 \leq N \leq N_{trunc}$ , where  $n_{trunc}$  and  $N_{trunc}$  are the minimum values of  $n$  and  $N$  for which the convergence is achieved. These numbers of photons and excited atoms are chosen sensibly larger than the average numbers of photons and excited atoms in the system. The physical parameters used in the calculations presented here are mainly dictated by computational considerations. Small transport mean free paths imply large hopping (cavity decay) rates compared with the atomic emission rate. This is accompanied by large numbers of photons in the system. These, in turn, lead to numerical convergence difficulties and a large number of equations. The Fano parameter calculated using the steady-state solutions of the truncated master equation (3.8) is presented in Fig. 6. In the example studied, the Fano parameter, obtained from a full nonadiabatic treatment, is enhanced relative to that given by the simpler Scully-Lamb theory. When the cavity decay rate is larger than the atomic relaxation rate, adiabatic elimination of the atomic variables leads to suppression of fluctuations. However, as shown in Fig. 7, the relative difference between the second-order correlation functions calculated using the two methods is not considerable above threshold. Moreover, the full master equation treatment leads to the same results as the Scully-Lamb theory regarding the dependence of fluctuations on the scatterers density, namely that the addition of scatterers into the system decreases the amount of fluctuations.

## VIII. CONCLUSIONS

Using a diffusion model with gain, obtained from a more general coherence propagation theory for the electric-field autocorrelation function, we have derived the generalized master equations for random-laser modes at different positions within the sample. Locally, these equations are formally

equivalent to that of a single-mode conventional laser with the cavity-loss terms replaced with terms that describe radiative transfer and multiple light scattering. We have shown that stronger scattering not only lowers the threshold for laser action, but also diminishes the noise with respect to the Poissonian value. These results may be used to explain the recent experiments, where, for a lower scatterer density [9], the radiation was found to be partially coherent, while for a system with stronger scatterers [10], the radiation became completely coherent above threshold. We have also shown that the intensity fluctuations increase with the gain concentration, and that light emitted deeper within the sample is more coherent than that emitted from near the front face of the sample.

The analysis presented here assumes isotropic scattering and uniform distribution of active molecules. It will be of considerable interest to extend this study to the case of anisotropic scattering and nonuniform, nonlinear gain concentration. In the case of nontrivial structure and nontrivial spatial correlations of the scattering particles, the scattering is anisotropic. This leads to a distinction between the scattering mean free path for photons and the transport mean free path. Also, as suggested in Sec. II, the statistical and spatial distributions of the gain medium lead to corrections to the classical diffusion coefficient, and thereby affect the coherence properties. A more general, nonlinear multiple-light-scattering theory is necessary to elucidate the coherence properties of the random laser and to fully describe the strong scattering regime of incipient photon localization ( $l^* \leq \lambda$ ) [33]. In this regime, our model suggests the possibility of enhanced coherence for the amplified light.

### ACKNOWLEDGMENT

This work was supported in part by the Natural Sciences and Engineering Research Council of Canada.

### APPENDIX A: THE DERIVATION OF THE DIFFUSION EQUATION

In this appendix, we derive the diffusion equation describing light propagation in an active random medium from radiative transfer theory.

Consider the transport equation (2.26) for the mean number of photons,  $\bar{n}_{\hat{\mathbf{k}}}(\mathbf{r}, t)$ , in the vicinity of a point  $\mathbf{r}$  and at time  $t$  and traveling in the direction of the wave vector  $\hat{\mathbf{k}}$ ,

$$\begin{aligned} \dot{\bar{n}}_{\hat{\mathbf{k}}}(\mathbf{r}) = & -c\hat{\mathbf{k}} \cdot \nabla \bar{n}_{\hat{\mathbf{k}}}(\mathbf{r}) + \sum_{\hat{\mathbf{k}}'} w_{\hat{\mathbf{k}}\hat{\mathbf{k}}'} [\bar{n}_{\hat{\mathbf{k}}'}(\mathbf{r}) - \bar{n}_{\hat{\mathbf{k}}}(\mathbf{r})] \\ & + \kappa [\bar{n}_{\hat{\mathbf{k}}}(\mathbf{r}) + 1] N(\mathbf{r}). \end{aligned} \quad (\text{A1})$$

Here,  $w_{\hat{\mathbf{k}}\hat{\mathbf{k}}'}$  is the elastic scattering rate,  $N(\mathbf{r})$  represents the number of excited atoms at position  $\mathbf{r}$ , and  $\kappa$  is the isotropic radiative rate.

One derives the diffusion equation from the transport equation (A1) by making the diffusion approximation, which consists in expanding  $\bar{n}_{\hat{\mathbf{k}}}(\mathbf{r})$  into spherical harmonics and keeping only the first two terms of the expansion [29]:

$$\bar{n}_{\hat{\mathbf{k}}}(\mathbf{r}) \approx \bar{n}(\mathbf{r}) + \frac{3}{c} \hat{\mathbf{k}} \cdot \mathbf{j}(\mathbf{r}). \quad (\text{A2})$$

Here,

$$\bar{n}(\mathbf{r}) = \sum_{\hat{\mathbf{k}}} \bar{n}_{\hat{\mathbf{k}}}(\mathbf{r}) \quad (\text{A3})$$

represents the total number of photons traveling in all directions, and the current density  $\mathbf{j}$  is defined by

$$\mathbf{j}(\mathbf{r}) = c \sum_{\hat{\mathbf{k}}} \hat{\mathbf{k}} \bar{n}_{\hat{\mathbf{k}}}(\mathbf{r}). \quad (\text{A4})$$

Here, we use the notation  $\Sigma_{\hat{\mathbf{k}}} \equiv (1/4\pi) \int d\hat{\mathbf{k}}$ .

The equation describing the evolution of the total number of photons,  $\bar{n}(\mathbf{r})$ , is obtained by summing over  $\hat{\mathbf{k}}$  in Eq. (A1). The terms corresponding to scattering sum to zero, and we obtain

$$\dot{\bar{n}}(\mathbf{r}) = -\nabla \cdot \mathbf{j}(\mathbf{r}) + \kappa [\bar{n}(\mathbf{r}) + 1]. \quad (\text{A5})$$

We now insert the expansion (A2) into the transport equation (A1), multiply the equation by  $\hat{\mathbf{k}}$ , and sum over  $\hat{\mathbf{k}}$ . We obtain

$$\frac{1}{c} \dot{\mathbf{j}}(\mathbf{r}) = -\frac{c}{3} \nabla \bar{n}(\mathbf{r}) - \frac{3}{c} \sum_{\hat{\mathbf{k}}, \hat{\mathbf{k}}'} \hat{\mathbf{k}} w_{\hat{\mathbf{k}}\hat{\mathbf{k}}'} (\hat{\mathbf{k}} - \hat{\mathbf{k}}') \cdot \mathbf{j}(\mathbf{r}) + \frac{1}{l_g} \mathbf{j}(\mathbf{r}). \quad (\text{A6})$$

Here,  $l_g^{-1} \equiv \kappa N(\mathbf{r})/c$  is the gain length. Using now that  $\Sigma_{\hat{\mathbf{k}}'} w_{\hat{\mathbf{k}}\hat{\mathbf{k}}'}$  is independent of  $\hat{\mathbf{k}}$  [see the definition (2.27)], and also that  $\Sigma_{\hat{\mathbf{k}}} \hat{\mathbf{k}} (\hat{\mathbf{k}} \cdot \mathbf{j}) = (1/3) \mathbf{j}$ , the first term in the sum on the right-hand side of Eq. (A6) becomes  $(1/3) \Sigma_{\hat{\mathbf{k}}'} w_{\hat{\mathbf{k}}\hat{\mathbf{k}}'} \mathbf{j}$ . On the other hand, using that  $\Sigma_{\hat{\mathbf{k}}} \hat{\mathbf{k}}' w_{\hat{\mathbf{k}}\hat{\mathbf{k}}'} = \Sigma_{\hat{\mathbf{k}}} \hat{\mathbf{k}} \cdot \hat{\mathbf{k}}' w_{\hat{\mathbf{k}}\hat{\mathbf{k}}'}$ , the second term in the sum on the right-hand side of Eq. (A6) becomes  $(1/3) \Sigma_{\hat{\mathbf{k}}} \hat{\mathbf{k}} \cdot \hat{\mathbf{k}}' w_{\hat{\mathbf{k}}\hat{\mathbf{k}}'} \mathbf{j}$ . Putting all these results together, Eq. (A6) becomes

$$\frac{1}{c} \dot{\mathbf{j}}(\mathbf{r}) = -\frac{c}{3} \nabla \bar{n}(\mathbf{r}) - \frac{1}{l^*} \mathbf{j}(\mathbf{r}) + \frac{1}{l_g} \mathbf{j}(\mathbf{r}). \quad (\text{A7})$$

Here,  $l^* = c\tau$  is the transport mean free path, related to the scattering properties of the medium by the scattering rate

$$\tau^{-1} \equiv \sum_{\hat{\mathbf{k}}'} w_{\hat{\mathbf{k}}\hat{\mathbf{k}}'} (1 - \hat{\mathbf{k}} \cdot \hat{\mathbf{k}}'). \quad (\text{A8})$$

Equations (A5) and (A7) represent the basic equations of the diffusion theory. By adiabatically eliminating the current  $\mathbf{j}$  from Eq. (A7), and inserting the corresponding expression into Eq. (A5), they are reduced to the diffusion equation

$$\dot{\bar{n}}(\mathbf{r}) = D \nabla_r^2 \bar{n}(\mathbf{r}) + \kappa \bar{N}(\mathbf{r}) [\bar{n}(\mathbf{r}) + 1]. \quad (\text{A9})$$

Here,  $D = c/3(1/l^* - 1/l_g)$  is the diffusion coefficient. For  $l^* \ll l_g$ , the diffusion coefficient becomes  $D = cl^*/3$ .

### APPENDIX B: THE DERIVATION OF TRANSPORT EQUATION FROM MASTER EQUATION

The equation obeyed by the average number of photons in the cell at  $\mathbf{r}$  and traveling in the direction of the wave vector

$$\begin{aligned} \dot{\bar{n}}_{\hat{\mathbf{k}}}(\mathbf{r}) = & -\kappa\{\overline{n_{\hat{\mathbf{k}}}(\mathbf{r})N(\mathbf{r})[n(\mathbf{r})+1]} - \overline{[n_{\hat{\mathbf{k}}}(\mathbf{r})+1]^2N(\mathbf{r})} - \overline{n_{\hat{\mathbf{k}}}(\mathbf{r})N(\mathbf{r})n(\mathbf{r})} + \overline{n_{\hat{\mathbf{k}}}^2(\mathbf{r})N(\mathbf{r})}\} + w\{-\overline{n_{\hat{\mathbf{k}}}(\mathbf{r})n(\mathbf{r})} + \overline{n_{\hat{\mathbf{k}}}(\mathbf{r})[n_{\hat{\mathbf{k}}}(\mathbf{r})-1]} \\ & + \overline{n_{\hat{\mathbf{k}}}(\mathbf{r})n(\mathbf{r})} - \overline{n_{\hat{\mathbf{k}}}^2(\mathbf{r})}\} + w\left[\overline{[\bar{n}_{\hat{\mathbf{k}}}(\mathbf{r})+1]\bar{n}_{\hat{\mathbf{k}}}(\mathbf{r}-\hat{\boldsymbol{\delta}}_{\hat{\mathbf{k}}})} + \bar{n}_{\hat{\mathbf{k}}}(\mathbf{r})\left(\sum_{\hat{\mathbf{k}}'\neq\hat{\mathbf{k}}}\bar{n}_{\hat{\mathbf{k}}}'(\mathbf{r}-\hat{\boldsymbol{\delta}}_{\hat{\mathbf{k}}}')\right) - \bar{n}_{\hat{\mathbf{k}}}(\mathbf{r})\left(\sum_{\hat{\mathbf{k}}'}\bar{n}_{\hat{\mathbf{k}}}'(\mathbf{r}-\hat{\boldsymbol{\delta}}_{\hat{\mathbf{k}}}')\right)\right] \\ & + \sum_{\hat{\mathbf{k}}'\neq\hat{\mathbf{k}}} w_{\hat{\mathbf{k}}\hat{\mathbf{k}}}'\left[-\bar{n}_{\hat{\mathbf{k}}}(\mathbf{r}) + \sum_{n_{\hat{\mathbf{k}}},n,N;\sum_{\hat{\mathbf{k}}'}n_{\hat{\mathbf{k}}}'=n} n_{\hat{\mathbf{k}}}n_{\hat{\mathbf{k}}}'(P_{\mathbf{r}}^{n_{\hat{\mathbf{k}}}-1,n,N} - P_{\mathbf{r}}^{n_{\hat{\mathbf{k}}},n,N})\right]. \end{aligned} \quad (\text{B1})$$

For isotropic scattering,  $w_{\hat{\mathbf{k}}\hat{\mathbf{k}}}' = W = \text{const}$ , and the last group of terms in Eq. (B1) can be written as

$$\begin{aligned} W \sum_{n_{\hat{\mathbf{k}}},n,N} n_{\hat{\mathbf{k}}}\{(n - (n_{\hat{\mathbf{k}}}-1))P_{\mathbf{r}}^{n_{\hat{\mathbf{k}}}-1,n,N} - n_{\hat{\mathbf{k}}}(n - n_{\hat{\mathbf{k}}})P_{\mathbf{r}}^{n_{\hat{\mathbf{k}}},n,N}\} \\ = W[\bar{n}(\mathbf{r}) - \bar{n}_{\hat{\mathbf{k}}}(\mathbf{r})] = \sum_{\hat{\mathbf{k}}'\neq\hat{\mathbf{k}}} W\bar{n}_{\hat{\mathbf{k}}}'(\mathbf{r}) = \sum_{\hat{\mathbf{k}}'\neq\hat{\mathbf{k}}} w_{\hat{\mathbf{k}}\hat{\mathbf{k}}}'\bar{n}_{\hat{\mathbf{k}}}'(\mathbf{r}). \end{aligned} \quad (\text{B2})$$

Equations (B1) and (B2) lead to

$$\begin{aligned} \dot{\bar{n}}_{\hat{\mathbf{k}}}(\mathbf{r}) = & \kappa\{\overline{[n_{\hat{\mathbf{k}}}(\mathbf{r})+1]N(\mathbf{r})} + w[-\bar{n}_{\hat{\mathbf{k}}}(\mathbf{r}) + \bar{n}_{\hat{\mathbf{k}}}(\mathbf{r}-\hat{\boldsymbol{\delta}}_{\hat{\mathbf{k}}})] \\ & + \sum_{\hat{\mathbf{k}},\hat{\mathbf{k}}'} w_{\hat{\mathbf{k}}\hat{\mathbf{k}}}'[\bar{n}_{\hat{\mathbf{k}}}'(\mathbf{r}) - \bar{n}_{\hat{\mathbf{k}}}(\mathbf{r})]. \end{aligned} \quad (\text{B3})$$

Using now the mean-field approximation  $\overline{n_{\hat{\mathbf{k}}}(\mathbf{r})N(\mathbf{r})} = \bar{n}_{\hat{\mathbf{k}}}(\mathbf{r})\bar{N}(\mathbf{r})$ , the expansion

$$\bar{n}_{\hat{\mathbf{k}}}(\mathbf{r}-\hat{\boldsymbol{\delta}}_{\hat{\mathbf{k}}}) \approx \bar{n}_{\hat{\mathbf{k}}}(\mathbf{r}) - \hat{\boldsymbol{\delta}}_{\hat{\mathbf{k}}}\cdot\nabla\bar{n}_{\hat{\mathbf{k}}}(\mathbf{r}), \quad (\text{B4})$$

(where  $\hat{\boldsymbol{\delta}}_{\hat{\mathbf{k}}} = l^*\hat{\mathbf{k}}$ ), and that  $w = c/l^*$ , Eq. (B3) takes the form (2.26).

### APPENDIX C

Using the expression (4.3), we obtain

$$f(0,\mathbf{r}) = \frac{\kappa\mathcal{N}(0,\mathbf{r})}{w} + \frac{D\nabla_{\mathbf{r}}^2\bar{n}(\mathbf{r}) + w\bar{n}(\mathbf{r})}{w}, \quad (\text{C1})$$

$\hat{\mathbf{k}}$ ,  $\bar{n}_{\hat{\mathbf{k}}}(\mathbf{r}) = \sum_{n_{\hat{\mathbf{k}}},n,N} n_{\hat{\mathbf{k}}}P_{\mathbf{r}}^{n_{\hat{\mathbf{k}}},n,N}$ , is obtained by multiplying the master equation (3.3) by  $n_{\hat{\mathbf{k}}}$  and summing over  $n_{\hat{\mathbf{k}}}$ ,  $n$  and  $N$ . The terms corresponding to relaxation processes and pump sum to zero, and we obtain:

where  $\mathcal{N}(0,\mathbf{r})$  can be obtained from Eq. (5.1) as

$$\mathcal{N}(0,\mathbf{r}) = \frac{\mathcal{P}(\mathbf{r})}{\gamma_{nr} + \kappa}. \quad (\text{C2})$$

On the other hand, the steady-state average number of excited atoms in the system,  $\bar{N}(\mathbf{r})$ , corresponding to the pumping rate  $\mathcal{P}(\mathbf{r})$  for which  $f(0,\mathbf{r}) = 1$  can be expressed as

$$\bar{N}(\mathbf{r}) = \frac{\mathcal{P}(\mathbf{r})}{\gamma_{nr} + \kappa[\bar{n}(\mathbf{r}) + 1]}. \quad (\text{C3})$$

Here,  $\bar{n}(\mathbf{r})$  is the average number of photons in the system. Using Eqs. (C2) and (C3), we can express  $\mathcal{N}(0,\mathbf{r})$  as

$$\mathcal{N}(0,\mathbf{r}) = \bar{N}(\mathbf{r})[1 + \beta\bar{n}(\mathbf{r})]. \quad (\text{C4})$$

Here,  $\beta \equiv \kappa/(\kappa + \gamma_{nr})$ .

According to the discussion presented in Sec. III, we have

$$|D\nabla_{\mathbf{r}}^2\bar{n}(\mathbf{r})| = \kappa\bar{N}(\mathbf{r})[\bar{n}(\mathbf{r}) + 1] \ll w\bar{n}(\mathbf{r}), \quad (\text{C5})$$

and also

$$\kappa\bar{N}(\mathbf{r})[1 + \beta\bar{n}(\mathbf{r})] < \kappa\bar{N}(\mathbf{r})[\bar{n}(\mathbf{r}) + 1] \ll w\bar{n}(\mathbf{r}). \quad (\text{C6})$$

As a result,  $\kappa\mathcal{N}(0,\mathbf{r})$  and  $D\nabla_{\mathbf{r}}^2\bar{n}(\mathbf{r})$  in Eq. (C1) can be neglected compared with  $w\bar{n}(\mathbf{r})$ , and  $f(0,\mathbf{r})$  can be approximated by

$$f(0,\mathbf{r}) \approx \bar{n}(\mathbf{r}). \quad (\text{C7})$$

Thus, the condition  $f(0,\mathbf{r}) = 1$  implies  $\bar{n}(\mathbf{r}) \approx 1$ .

- [1] V.S. Letokhov, Zh. Éksp. Teor. Fiz **53**, 1442 (1967) [Sov. Phys. JETP **26**, 835 (1968)].  
 [2] N.M. Lawandy *et al.*, Nature (London) **368**, 436 (1994).  
 [3] W.L. Sha, C.-H. Liu, and R.R. Alfano, Opt. Lett. **19**, 1922 (1994).  
 [4] D.S. Wiersma, M.P. van Albada, and Ad. Lagendijk, Nature

- (London) **373**, 203 (1995).  
 [5] N.M. Lawandy and R.M. Balachandran, Nature (London) **373**, 204 (1995).  
 [6] M. Siddique, R.R. Alfano, G.A. Berger, M. Kempe, and A.Z. Genack, Opt. Lett. **21**, 450 (1996).  
 [7] H. Cao, Y.G. Zhao, S.T. Ho, E.W. Seelig, Q.H. Wang, and

- R.P.H. Chang, Phys. Rev. Lett. **82**, 2278 (1999).
- [8] G.R. Williams, S.B. Bayram, S.C. Rand, T. Hinklin, and R.M. Laine, Phys. Rev. A **65**, 013807 (2002).
- [9] G. Zacharakis, N.A. Papadogiannis, G. Filippidis, and T.G. Papazoglou, Opt. Lett. **25**, 923 (2000).
- [10] H. Cao, Y. Ling, J.Y. Xu, C.Q. Cao, and P. Kumar, Phys. Rev. Lett. **86**, 4524 (2001).
- [11] S. John and G. Pang, Phys. Rev. A **54**, 3642 (1996).
- [12] G.A. Berger, M. Kempe, and A.Z. Genack, Phys. Rev. E **56**, 3462 (1997).
- [13] X. Jiang and C.M. Soukoulis, Phys. Rev. Lett. **85**, 70 (2000).
- [14] M. Sargent, III, M.O. Scully, and W.E. Lamb, Jr., *Laser Physics* (Addison-Wesley, Reading, MA, 1974).
- [15] A.Yu. Zyuzin, Phys. Rev. E **51**, 5274 (1995).
- [16] C.W.J. Beenakker, Phys. Rev. Lett. **81**, 1829 (1998).
- [17] G. Hackenbroich, C. Viviescas, B. Elattari, and F. Haake, Phys. Rev. Lett. **86**, 5262 (2001).
- [18] M. Patra, Phys. Rev. A **65**, 043809 (2002).
- [19] P.R. Rice and H.J. Carmichael, Phys. Rev. A **50**, 4318 (1994).
- [20] V.M. Apalkov, M.E. Raikh, and B. Shapiro, Phys. Rev. Lett. **89**, 016802 (2002).
- [21] L. Mandel, Phys. Rev. **136**, B1221 (1964).
- [22] A.E. Siegman, *Lasers* (University Science Books, Sausalito, CA, 1986).
- [23] F.C. MacKintosh and S. John, Phys. Rev. B **40**, 2383 (1989).
- [24] We have [22]  $\chi_0 = |\mathbf{d}|^2 / \hbar (\Delta\omega + i/T_2)$ , where  $|\mathbf{d}|^2$  is the dipole matrix element for the atomic laser transition,  $\Delta\omega \equiv \omega - \omega_a$  is the frequency detuning ( $\omega_a$  is the central frequency of the gain profile), and  $T_2$  is the dipole relaxation time. The saturation intensity is given by  $I_{sat} = \hbar^2/4|\mathbf{d}|^2 T_1 T_2$ , where  $T_1$  is the atomic excited state lifetime.
- [25] S. John, G. Pang, and Y. Yang, J. Biomed. Opt. **1**, 180 (1996).
- [26] S. John and M.J. Stephen, Phys. Rev. B **28**, 6358 (1983).
- [27] D. Vollhardt and P. Wölfle, Phys. Rev. Lett. **45**, 842 (1980); D. Vollhardt and P. Wölfle, Phys. Rev. B **22**, 4666 (1980).
- [28] H.T. Nieh, L. Chen, and P. Sheng, Phys. Rev. E **57**, 1145 (1998).
- [29] K.M. Case and P.W. Zweifel, *Linear Transport Theory* (Addison-Wesley, Reading, MA, 1967).
- [30] K. Busch (unpublished).
- [31] R.P. Feynman, R.B. Leighton, and M. Sands, *The Feynman Lectures on Physics*, Vol. 3 (Addison-Wesley, Reading, MA, 1965).
- [32] For a more general study of the decay rates of a disordered slab, see M. Patra, Phys. Rev. E **67**, 016603 (2003).
- [33] S. John, Phys. Rev. Lett. **53**, 2169 (1984).
- [34] H.J. Carmichael, *Statistical Methods in Quantum Optics I* (Springer-Verlag, Berlin, 1999).
- [35] L. Mandel, Opt. Commun. **42**, 356 (1982).
- [36] R. Loudon, *The Quantum Theory of Light* (Oxford University Press, Oxford, 2002).
- [37] In the case when the system is pumped from the front side and the emission is measured from the side windows (see Refs. [4,5]), the pumping rate is constant in the transverse (side) direction, and  $L$  should be replaced by the actual length of the sample in the transverse (side) direction.
- [38] E. Akkermans, P.E. Wolf, and R. Maynard, Phys. Rev. Lett. **56**, 1471 (1986).